

# **Development of Biomimetic Approaches for Immunoisolation of Functional Islets**

by

**Mükrimе Birgöl Akolpođlu**

A Thesis Submitted to the  
Graduate School of Sciences and Engineering  
in Partial Fulfillment of the Requirements for  
the Degree of  
Master of Science  
in  
Chemical and Biological Engineering



**KOÇ  
UNIVERSITY**

September 2018

**Development of Biomimetic Approaches for  
Immunoisolation of Functional Islets**

Koç University  
Graduate School of Sciences and Engineering

This is to certify that I have examined this copy of a master's thesis by

**Mükrime Birgül Akolpoğlu**

and have found that it is complete and satisfactory in all respects,  
and that any and all revisions required by the final  
examining committee have been made.

Committee Members:

---

Assoc. Prof. Seda Kızılel

---

Asst. Prof. Cem Albayrak

---

Assoc. Prof. Sezen Soyer Uzun

Date: \_\_\_\_\_



*To my mother  
and to my father and sister,*

## **ABSTRACT**

Type 1 diabetes (T1D) is a chronic autoimmune disease of pancreas, where insulin secretion function is lost due to destruction of insulin secreting  $\beta$  cells. People with T1D have high blood glucose levels, while their cells are deprived from glucose for their metabolic actions. Islets are “islands of  $\beta$  cells” and responsible for glucose metabolism in the body. Islet transplantation has transitioned from an experimental and occasionally-employed strategy to a routine clinical therapy for T1D in the past decade. Nevertheless, lifelong immunosuppression and the necessity of multiple transplantations limit wider application of this strategy. Islet immunoisolation techniques have emerged to eliminate immunosuppression permanently or to reduce immunosuppressive drug doses significantly. The concept of immunoisolation is to create a local secure microenvironment for islets to prevent graft rejection. Regulation of immune system can be done by several material-based and biologic strategies. While material-based strategies focus on preserving islets within semi-permeable membranes that allow nutrient exchange and block immune system components, biological strategies deal with regulation of immune system through chemokines and manipulation of immune cells. This thesis focuses on two of those strategies to create tolerable grafts and overcome islet graft rejection. We firstly engineered pseudoislets, or islet organoids, that are composed of insulin secreting  $\beta$  cells ( $\beta$ -TC-6) and hepatic stellate cells (HSCs). HSCs have the ability to secrete ECM proteins, angiogenesis factors and expand regulatory T cell (Treg) population in their vicinity. Tregs are crucial in modulating the immune system by suppressing and downregulating actions of effector T cells. A macrophage derived chemokine, CCL22, also has the ability to recruit Tregs and provide a local immunosuppression. We combined these two concepts and transfected Tregs with CCL22 gene. Then we prepared insulin-secreting multicellular organoids with  $\beta$ -TC-6 and CCL22-transfected HSCs. Implantation of these multicellular organoids to diabetic animal model resulted in more than 5-fold increase in Treg recruitment towards implantation site. This result suggested that tolerable grafts could be

fabricated through modulation of the immune system not only for islet therapy but also for other cell/organ transplantation therapies. To create another type of immunoisolation for islets, we also designed biocompatible hydrogels and formed ultra-thin coatings around islet organoids. Lipid group bearing microgels were synthesized by water-in-water emulsion (W/W) followed by photopolymerization steps. We optimized microgel diameter by changing emulsion and photopolymerization parameters. The smallest microgel diameter (2,13  $\mu\text{m}$ ) was achieved at 60% ultrasonication power for 30 minutes. In W/W emulsion and photopolymerization steps, each reaction step was carried out in aqueous solutions at physiological pH values. We prepared  $\beta$ -TC-6 organoids by hanging drop method and deposited lipid-microgels on organoid surface via non-covalent hydrophobic interactions. Unlike covalent bonding, hydrophobic interactions between lipid functionalities in our microgels and phospholipid bilayer on cell membranes present no harm to cells. Hydrophobic interactions do not damage membrane proteins and perturb the integrity of the membrane. We studied the coating of microgels with two different lipid concentrations, 2.5 and 5 mM. Furthermore, we coated islet organoids with two different microgel concentrations, 10 and 20 mg/ml. We observed that coating efficiency was higher when lipid concentration was increased due to more hydrophobic interactions. We obtained high and similar metabolic activity and viability for microgel coated islet organoids compared to non-coated controls. Insulin secretion functionality was also preserved, meaning that our approach of immunoisolation allowed us to engineer functional insulin secreting organoids. Our findings suggest that biological and material-based immunotherapeutic strategies hold great potential for islet transplantation in T1D treatment.

## ÖZET

Tip 1 diyabet (T1D), insülin salgılayan  $\beta$  hücrelerinin yıkımı nedeniyle insülin salgılama fonksiyonunun kaybedildiği, pankreasın kronik bir otoimmün hastalığıdır. T1D hastaları yüksek kan glukoz seviyelerine sahipken, hücreleri glukozdan mahrumdur. Adacıklar “ $\beta$  hücreleri adaları” diye tanımlanabilir ve vücuttaki glikoz metabolizmasından sorumludurlar. Adacık transplantasyonu, son on yıl içerisinde T1D için deneysel ve zaman zaman uygulanan bir stratejiden rutin olarak uygulanan klinik terapiye dönüşmüştür. Fakat, ömür boyu bağışıklık sistemi baskılayıcı ilaç kullanma ve bir seferden fazla adacık nakli gerekliliği bu stratejinin daha geniş bir alanda uygulanmasını sınırlamaktadır. Adacık immünoizolasyon teknikleri, bağışıklık sistemini baskılamak için ilaç kullanma gerekliliğini kalıcı olarak ortadan kaldırılması veya ilaç dozlarının önemli ölçüde azaltılması için ortaya çıkmış tekniklere verilen genel bir addır. Bağışıklık sisteminin düzenlenmesi çeşitli malzeme bazlı ve biyolojik stratejilerle yapılabilir. Malzeme bazlı stratejiler, adacıkları besin değişimini sağlayan ve bağışıklık sistemi bileşenlerini bloke eden yarı geçirgen membranlar içinde alarak adacıkların korunmasına odaklanırken; biyolojik stratejiler, bağışıklık sisteminin kemokinler yoluyla veya bağışıklık hücrelerinin manipülasyonu ile düzenlenmesiyle ilgilenir. Bu tez, tolere edilebilir adacık nakillerinin yaratılması ve adacık reddinin üstesinden gelmek için bu iki stratejiye odaklanmaktadır. İlk olarak insülin salgılayan  $\beta$  hücreleri ( $\beta$ -TC-6) ve hepatik stellat hücrelerinden (HSC'ler) oluşan yalancı adacıklar veya adacık organoidlerini tasarladık. HSC'ler ECM proteinlerini ve anjiyogenez faktörlerini salgılayabilir ve aynı zamanda yakın çevrelerindeki düzenleyici T hücresi (Treg) popülasyonunu genişletebilirler. Tregler, efektör T hücrelerinin faaliyetlerini baskılayarak bağışıklık sistemini modüle etmede çok önemlidir. Makrofajlardan türetilmiş bir kemokin olan CCL22 da Treg çağırma ve dolayısıyla lokal bir bağışıklık baskılama yeteneğine sahiptir. Çalışmamızda bu iki kavramı birleştirdik ve Treg'leri CCL22 geni ile transfekte ettik. Daha sonra,  $\beta$ -TC-6 ve CCL22 ile transfekte edilmiş HSC'ler ile insülin salgılayan çok hücreli organoidler hazırladık. Bu çok hücreli organoidlerin diyabetik hayvan modeline implantasyonu neticesinde, implantasyon bölgesindeki Treg sayısında 5 kattan fazla artış olduğunu gözlemledik. Bu sonuç, tolere edilebilir adacık nakillerinin, sadece adacık tedavisi

için değil aynı zamanda diğer hücre/organ transplantasyonları için de bağışıklık sisteminin modülasyonu yoluyla üretilebileceğini gösterdi. Adacıklar için başka bir immünoizolasyon türü yaratmak için, biyouyumlu hidrojel tasarladık ve adacık organoidlerinin etrafında ultra-ince kaplamalar oluşturduk. Lipid grubu barındıran mikrojeller, su içinde su emülsiyon tekniği ve ardından fotopolimerizasyon ile sentezlendi. Her bir reaksiyon aşaması, fizyolojik pH değerlerinde sulu çözeltilerde gerçekleştirildi. Mikrojeller hidrofobik etkileşimler yoluyla organoid bağlandı. Kovalent bağlanmadan farklı olarak, hidrofobik etkileşimler hücre yüzeyinde bulunan membrane proteinleri ile etkileşime girmez ve hücre zarının bütünlüğünü bozmaz. Kaplanmamış kontrollere kıyasla mikrojel kaplı adacık organoidleri için yüksek ve benzer hücre metabolik aktivite ve canlılık değerleri elde ettik. Adacıkların insülin salgılama kapasiteeri incelendiğinde, mikrojellerle kaplanmış adacıklar ve kaplanmamış adacıklar arasında büyük farklılıklar gözlenmemiş, böylelikle insülin salgılama işlevselliği de korunmuştur. Edindiğimiz sonuçlar, immünoizolasyon yaklaşımımız aracılığıyla, fonksiyonel insülin salgılayan organoidlerin üretilebileceğini bize göstermektedir. Bulgularımız biyolojik ve materyal bazlı immünoterapötik stratejilerin T1D tedavisinde adacık nakli için büyük bir potansiyel taşıdığını göstermektedir.

## ACKNOWLEDGEMENTS

Foremost, I would like to take this opportunity to wholeheartedly express my gratitude to my advisor, Assoc. Dr. Seda Kızılel for guiding, encouraging and believing in me. You have been a role model for me, a successful scientist woman in her field, and an excellent mentor. Thanks to you, I had the opportunity to do research in a field which I have been curious about ever since I was a child. I have always admired how you managed your time and how you kept track of the newest advancements in your field. Your enthusiasm, creative thinking and ambition will always be there with me and I will always keep challenging myself to become a scientist like you.

Special thanks to Assoc. Prof Sezen Soyer Uzun and Asst. Prof Cem Albayrak for serving as my committee members and sparing their valuable time for evaluation of my thesis.

I would like to thank my past lab mates Dilem, Pelin, Derya and Tuğba. I owe them a lot, for showing me how things work around the lab, for training me and sharing their unique experience and knowledge with me. I will absolutely miss all the professional and social harmony we had. I am especially grateful for Dilem's friendship outside the lab and being so kind and sweet. I would also like to thank my present lab mates, Yasemin and Rubab. Yasemin and I have been through many challenges together and I cherish every scientific discussion we had together. Apart from that, I am lucky to have her as a friend who is always supportive and always fun to spend time with.

I would like to thank my dearest friend, Eda Kolatu. She is "the" most positive, loving, supportive, passionate and kind person I have ever seen. She always knows how to cheer me up. Even though we have been miles away from each other physically, we are forever together in spirit.

Sinem Apaydın is someone I met only 1,5 years ago and I swear it feels like I know her for 15 years. I will never forget our cooking sessions, dinner parties, coffee breaks and cat-petting sessions. Even though you are overseas now, I know

that this means nothing to us, because we are masters of friendship (and science now).

I also would like to thank Uğur for being yourself. You have always been so loving, caring, so kind and generous. Thank you for always making me laugh. Thank you for all your support. Thank you for your love. I can't imagine my life without you and I am looking forward to our next adventure.

And finally, I would like to thank my amazing family, my mom Ayşegül, my dad Vahap and my sister İdil. My İdil, my best friend, my everything. Thank you for being the bigger sister when I can't think through. You are such an inspiration for me. I love you so very much. Thank you for loving me back unconditionally. Mom and dad, thank you for your endless support physically and mentally. You guys have been my rock. I cannot thank you enough for all the sacrifice you have made so that me and my sister can get a decent education and become independent women. Especially you mom, I am eternally proud of you, I hope I can make you proud, too.

## TABLE OF CONTENTS

<b>LIST OF TABLES .....</b>	<b>xii</b>
<b>LIST OF FIGURES .....</b>	<b>xiii</b>
<b>NOMENCLATURE .....</b>	<b>xvi</b>
<b>Chapter 1: Introduction .....</b>	<b>1</b>
<b>Chapter 2: Literature Review .....</b>	<b>4</b>
2.1. Type 1 diabetes .....	4
2.2 Current Treatment Strategies for T1D .....	5
2.2.1. Insulin Therapy .....	6
2.2.2. Pancreas Transplantation .....	6
2.2.3. Islet Transplantation .....	7
2.3 Islet Engineering .....	8
2.3.1. Formation of $\beta$ Cell Organoids .....	8
2.3.2. Prevention of Islet Graft Failure .....	10
2.3.2.1. Cell-based Methods .....	10
2.3.2.2. Material-based Methods .....	12
2.4 Water-in-water (W/W) Emulsions .....	17
2.4.1. Preparation and Stabilization of W/W Emulsions .....	18
2.4.2. Applications of W/W Emulsions .....	18
2.4.3. PEG Hydrogel Particles .....	19
<b>Chapter 3: Recruitment of Regulatory T Cells to Implant Site in Islet Transplantation by Beta-Stellate Cell Organoids .....</b>	<b>20</b>
3.1. Introduction .....	20
3.2 Experimental .....	22
3.2.1 Cell Culture .....	22
3.2.2 Plasmid constructs .....	22
3.2.3 Virus Production and Infection of Hepatic Stellate Cells .....	23
3.2.4 CCL22 Protein Determination .....	23
3.2.5. Multicellular Organoid Formation by Hanging Drop .....	23
3.2.6. Transplantation of Multicellular Organoids to Diabetic Mice .....	24
3.2.7 Flow Cytometry .....	25
3.3. Results and Discussion .....	26
3.3.1 Confirmation for CCL22 Transfection with ELISA Assay .....	26
3.3.2 Recruitment of Tregs in Diabetic Animal Model .....	26

3.4. Conclusion and Future Work .....	29
<b>Chapter 4: Coating of Insulin Secreting <math>\beta</math>-cell Organoids with Lipid Containing Microgels .....</b>	<b>31</b>
4.1. Introduction .....	31
4.2. Experimental .....	34
4.2.1. Preparation of PEG Hydrogel Prepolymer Solutions .....	34
4.2.2. Microgel Synthesis .....	34
4.2.3. Visualization of Microgels .....	36
4.2.4. Cell Culture .....	36
4.2.5. $\beta$ -TC-6 Islet Organoid Formation.....	36
4.2.6. Coating of $\beta$ -TC-6 Organoids With PEG-Lipid Microgels.....	36
4.2.7. Viability of Microgel Coated $\beta$ -TC-6 Organoids .....	37
4.2.8. Metabolic Activity of Microgel Coated $\beta$ -TC-6 Organoids ....	38
4.2.9. Functionality of Microgel Coated $\beta$ -TC-6 Organoids .....	38
4.3. Results and Discussion.....	39
4.3.1. PEG Microgel Synthesis by Water-in-Water (W/W) Emulsion and Photopolymerization .....	39
4.3.1.1 Effect of Ultrasonication on Microgel Diameter .....	39
4.3.1.2 Effect of Laser Exposure Time on Microgel Formation....	43
4.3.1.3. Morphology and Fluorescent Labeling of PEG Microgels	48
4.3.2. $\beta$ -TC-6 Organoid Formation with Hanging Drop and Coating of Organoids with Lipid-containing Microgels.....	51
4.3.4. Viability of Coated $\beta$ -TC-6 Organoids.....	53
4.3.5. Metabolic Activity of Coated $\beta$ -TC-6 Organoids.....	54
4.3.6. Insulin Secretory Function of Coated $\beta$ -TC-6 Organoids .....	56
<b>Chapter 5: Conclusions and Future Work .....</b>	<b>58</b>
<b>BIBLIOGRAPHY .....</b>	<b>60</b>

## LIST OF TABLES

<b>Table 2. 1.</b> Guidelines for the diagnosis of diabetes .....	4
---	---



## LIST OF FIGURES

<b>Figure 2. 1.</b> Treatment strategies for T1D. (a) islets derived from stem cell differentiation. (b) co-transplantation or co-culture of islets/beta cells with other cell types. (c) islet transplantation with biomaterials such as hydrogel scaffolds. (d) pancreas transplantation. (e) isolated islet transplantation. (f) insulin therapy.....	6
<b>Figure 2. 2.</b> Methods for $\beta$ cell organoid formation.....	9
<b>Figure 2. 3.</b> Immunoisolation of islets with biomaterials.....	13
<b>Figure 2. 4.</b> Chemical structures of the most commonly used polymers as immunoprotective barriers for islet transplantation. (a) alginate. (b) agarose. (c) poly (ethylene glycol) (PEG). (d) chitosan. ....	14
<b>Figure 2. 5.</b> Islet coating strategies.....	16
<b>Figure 2. 6.</b> Schematics for W/W emulsions.....	17
<b>Figure 3. 1.</b> Preparation of multicellular organoids by hanging drop method .....	24
<b>Figure 3. 2.</b> 600 multicellular organoids were implanted to diabetic mice. Tissues were retrieved from animals at day 10 for flow cytometry analysis.....	25
<b>Figure 3. 3.</b> Expression of CCL22 by transduced HSCs. Protein concentrations were quantified with CCL22 ELISA kit. ....	26
<b>Figure 3. 4.</b> Flow cytometry analysis results for PBS-treated control animals. 100 $\mu$ L PBS was injected into left abdominal external oblique muscle of STZ-induced diabetic mice. Tissues from implant site and a control site was retrieved 10 days after the procedure. Treg flow assay was performed to determine Treg recruitment by analyzing CD4+CD25+FoxP3+ cells. (a, c, e, g) Flow analysis results from control tissues and (b, d, e,f) Flow analysis results from implant tissue. ....	27
<b>Figure 3. 5.</b> Flow cytometry analysis results for organoid-implanted animals. 600 multicellular organoids of $\beta$ -TC-6:HSC-CCL22 were implanted to STZ-induced diabetic mice. Tissues from implant site and a control site was retrieved 10 days after the procedure. Treg flow assay was performed to determine Treg recruitment by analyzing CD4+CD25+FoxP3+ cells. (a, c, e, g) Flow analysis results from control tissues and (b, d, e,f) Flow analysis results from implant tissue. ....	28
<b>Figure 3. 6.</b> Treg recruitment in vivo. % FoxP3+ cells in CD4+ cell population indicates presence of Tregs in the tissues. ....	29
<b>Figure 4. 1.</b> Microgel synthesis by W/W emulsion.....	35
<b>Figure 4. 2.</b> $\beta$ -TC-6 organoid formation and coating of organoids. A) Organoid formation by hanging drop technique. B) Coating of organoids with fluorescently-labeled microgels at various concentrations (10 and 20 mg/mL). ....	37
<b>Figure 4. 3.</b> Microscope images of PEG microgels prepared by emulsification at 30% homogenizer power. Images were captured after laser exposure. Insets represent size distribution histograms of microgels. Size distributions were calculated by Image J using microscope images at 20x magnification. ....	40

<b>Figure 4. 4.</b> Microscope images of PEG microgels prepared by emulsification at 60% homogenizer power. Images were captured after laser exposure. Insets represent size distribution histograms of microgels. Size distributions were calculated by Image J using microscope images at 20x magnification. ....	41
<b>Figure 4. 5.</b> Microgel diameters after tuning ultrasonication parameters. ....	42
<b>Figure 4. 6.</b> Microscope images of photopolymerized PEG microgels. Laser duration = 1 minute. Images were captured right after laser exposure. 4 consecutive images of the same area were captured at different time points (0, 30, 60 and 180 seconds). Scale bar= 100µm. ....	44
<b>Figure 4. 7.</b> Microscope images of photopolymerized PEG microgels. Laser duration = 1,5 minutes. Images were captured right after laser exposure. 4 consecutive images of the same area were captured at different time points (0, 30, 60 and 180 seconds). Scale bar= 100µm. ....	45
<b>Figure 4. 8.</b> Microscope images of photopolymerized PEG microgels. Laser duration = 2,5 minutes. Images were captured right after laser exposure. 4 consecutive images of the same area were captured at different time points (0, 30, 60 and 180 seconds). Scale bar= 100µm. ....	46
<b>Figure 4. 9.</b> Demonstration of the effect of laser exposure on microgel formation. If sufficient energy is transferred to emulsions during photopolymerization, stable microgels are obtained, while insufficient energy causes micro-droplets to burst and disappear since crosslinking efficiency is low. ....	47
<b>Figure 4. 10.</b> Microscope images of photopolymerized PEG microgels. Laser duration = 3 and 3,5 minutes. Images were captured right after laser exposure. Scale bar= 100 µm. ....	48
<b>Figure 4. 11.</b> FE-SEM images of PEG microgels synthesized with different ultrasonication power densities and durations. Scale bar= 2 µm. ....	49
<b>Figure 4. 12.</b> Brightfield and fluorescent images of PEG microgels synthesized with optimized ultrasonication and laser exposure parameters (60% power, 30 min ultrasonication and 2,5 min laser exposure). Images were captured before and after washing microgels. (a, b) before, (c,d) after washing. Scale bars for a and b = 10 µm, c and d =5 µm. ....	50
<b>Figure 4. 13.</b> Confirmation of fluorescent conjugation to microgels. Fluorescein-o-acrylate was added to microgels after laser exposure as control group. Fluorescence signal fades in control microgels, whereas the signal remains in labeled microgels. ....	50
<b>Figure 4. 14.</b> Chemical structure of acrylate-PEG-DSPE .....	51
<b>Figure 4. 15.</b> Schematic representation of the hydrophobic interaction between PEG-lipid microgels and phospholipid bilayer on cell membrane. ....	52
<b>Figure 4. 16.</b> PEG-lipid microgel coating of β-TC-6 organoids with different microgel and lipid concentrations. A) Fluorescence images of coated organoids. Scale bars=100µm. B) surface area and C) diameter of islet organoids. ....	53
<b>Figure 4. 17.</b> Live/dead staining of β-TC-6 organoids after microgel coating. Green: Viable (fluorescein diacetate). Red: Dead (propidium iodide). Scale bars=100µm. ....	54

**Figure 4. 18.** Metabolic activity of  $\beta$ -TC-6 organoids after microgel treatment. A) ATP levels. B) Percent viabilities and C) Caspase activity of organoids. Percent viabilities and caspase activities were calculated by normalizing values of coated groups to non-coated control group. .... 55

**Figure 4. 19.** Stimulation indices of  $\beta$ -TC-6 organoids after microgel treatment. SI values were calculated by dividing insulin level at high glucose to insulin level in low glucose buffer. .... 56



## NOMENCLATURE

ATPS	Aqueous two-phase systems
BG	Blood glucose
CAMs	Cell adhesion molecules
CCL22	Chemokine C-C motif ligand 22
CHPOA	Cholesterol bearing pullulan
ECM	Extracellular matrix
FDA	Fluorescein diacetate
FoxP3	Forkhead box P3
GLP-1	Glucagon like peptide-1
HGF	Hepatocyte growth factor
HSCs	Hepatic stellate cells
IBMIR	Instant blood-mediated inflammatory responses
IL10	Interleukin 10
iPSC	Induced pluripotent stem cells
MIN6	Mouse insulinoma 6
MSCs	Mesenchymal stem cells
PEG	Poly (ethylene glycol)
PEGDA	Poly (ethylene glycol) diacrylate
PI	Propidium iodide
PSC	Pancreatic stellate cells
RCCS	Rotational cell culture systems
RINm5F	Rat insulinoma 5
SCs	Stellate cells
STZ	Streptozotocin
T1D	Type 1 diabetes
T2D	Type 2 diabetes
TGF- $\beta$	Growth factor- $\beta$
Tregs	Regulatory T cells
VEGF	Vascular endothelial growth factor
W/W	Water-in-water emulsion

## Chapter 1 INTRODUCTION

Diabetes is a chronic disease precipitated by genetic, environmental and life-style related reasons. It is categorized into 4 types by The American Diabetes Association: Type 1 diabetes (T1D), Type 2 diabetes (T2D), gestational diabetes and other specific types of diabetes such as drug or chemical-induced diabetes [1]. Among these diabetes types, T1D accounts for 5-10% of all diabetic patients.

T1D is caused by  $\beta$  cell destruction in pancreas.  $\beta$  cells exist in clusters called islets and they constitute 2-3% of pancreas [2]. After the destruction of  $\beta$  cells, insulin deficiency occurs, which means that Type 1 diabetic patients cannot secrete insulin. Insulin is a hormone required for glucose to enter our cells and generate energy for cellular activities. Although glucose is abundant in their body, patients with T1D cannot make use of it, while their cells are starving for glucose.

The most available treatment option for T1D is insulin therapy. Insulin is delivered to patients' blood stream through daily multiple injections, which is an exhaustive treatment and is not a cure but rather a relief therapy. Other treatment options include pancreas and islet transplantation. Pancreas transplantation is preferred for the patients with end-stage diabetes, where insulin is required for their survival and insulin injections do not cover their needs anymore [3]. It is a risky operation and lack of donor limits its wider practice in the clinical setting. On the other hand, islet transplantation is carried out by simply infusing islets to patient's liver through a percutaneous catheter [4]. Nevertheless, after both transplantations, host body does not identify the organ/islet as its own, therefore creates an immune response by attacking to the newly implanted graft. To overcome immune reactions, patients receive immunosuppressive drug treatment, most commonly sirolimus and tacrolimus administration [5]. However, long-term immunosuppression has severe adverse effects on both the functionality of implanted islets and on patient's body. For instance, sirolimus administration causes very serious side effects, including mouth ulcers, nephrotoxicity, anemia and hypercholesterolemia [6]. Therefore, it is

arguable whether receiving an organ transplant ameliorates patients' life quality or not.

Several strategies have emerged in the past three decades to solve the problems related to the need for immunosuppression. For example, encapsulation or coating islets within permselective membranes, which protects them from immune attacks, is the most commonly investigated approach for islet transplantation. The most important factors in biomaterial selection for islet coating are biocompatibility, availability, simple production steps and mild coating steps. Once coated, islets are immunoisolated from their environment, whereas they are able to receive nutrient/oxygen and diffuse out their waste products, signaling factors and hormones (e.g. insulin). Thickness of the coating material is critical, since for a convenient islet transplantation procedure, the volume of transplant should not exceed a certain limit. Especially, microencapsulation and ultra-thin coating of islets have the benefit of low transplant volume [7]. Another approach for creating immunoisolation is done by regulating the immune system itself by manipulating its own components. For example, regulatory T cells (Tregs) are responsible for the suppression of the immune system by blocking T cell activity. Gołab et al. coated pancreatic islets with Tregs and reported that islet function was preserved [8]. Islet co-transplantation with companion cells, such as mesenchymal stem cells, (MSCs), endothelial cells and stellate cells (SCs), may overcome problems related to islet rejection through making use of regulatory and vasculogenic functions of such cells [9-11].

In this thesis study, we designed local secure microenvironments for islet grafts through cell-based and material-based strategies. We studied the interactions between insulin secreting  $\beta$ -cells and stellate cells and designed insulin-secreting islet organoids with optimum viability and function. As a next step, we prepared and optimized microgels and performed microgel coating of islet organoids.

An outlook on the development of T1D and its current treatment options are presented in Chapter 2. Cell- and material-based strategies to overcome islet graft rejection were also summarized.

In Chapter 3, we formed multicellular islet organoids composed of insulin-secreting  $\beta$ -TC-6 cells and HSCs. HSCs were transfected with CCL22 gene for Treg recruitment. This *in vivo* study showed us that Treg population around islet implants can be expanded and islet graft tolerance can be obtained by this approach.

To take our research one step forward, we designed fully-biocompatible microgel particles with lipid functionality and performed islet coating experiments in Chapter 4. PEG-lipid microgels were synthesized by water in water emulsion method (W/W), followed by photopolymerization. Different parameters effecting microgel diameter and formation was thoroughly investigated and presented.

Finally, conclusions and future work related to our study was summarized in Chapter 5.

To the best of our knowledge, both of our concepts have not been studied extensively in the literature and hold great potential for immunoisolation of islets grafts for enhancing islet transplantation therapy in T1D.

Chapter 2  
**LITERATURE REVIEW**

**2.1. Type 1 diabetes**

Type 1 diabetes (T1D) is an immune-associated chronic disease of pancreas. T1D is characterized by the destruction of  $\beta$  cells in the pancreatic islets of Langerhans. Islets of Langerhans constitute the endocrine tissue of the pancreas and they contain  $\alpha$ ,  $\beta$ ,  $\delta$  and PP cells, among which  $\beta$  cells are responsible for insulin secretion [12]. Insulin secretion ability is declined in Type 1 diabetic patients because of  $\beta$  cell destruction. Since insulin regulates blood glucose concentration, these patients have high blood glucose levels.

**Table 2. 1.** Guidelines for the diagnosis of diabetes [1]

1. A1C $\geq 6.5\%$ . The test should be performed in a laboratory using a method that is NGSP certified and standardized to the DCCT assay.*
OR
2. FPG $\geq 126$ mg/dl (7.0 mmol/l). Fasting is defined as no caloric intake for at least 8 h.*
OR
3. 2-h plasma glucose $\geq 200$ mg/dl (11.1 mmol/l) during an OGTT. The test should be performed as described by the World Health Organization, using a glucose load containing the equivalent of 75 g anhydrous glucose dissolved in water.*
OR
4. In a patient with classic symptoms of hyperglycemia or hyperglycemic crisis, a random plasma glucose $\geq 200$ mg/dl (11.1 mmol/l).

\*In the absence of unequivocal hyperglycemia, criteria 1–3 should be confirmed by repeat testing.

Diabetes is diagnosed by fasting blood glucose level of 7 mmol/L (126 mg/dL) or higher and in general, blood glucose level higher than 11.1 mmol/L (200

mg/dL). Test guidelines for the diagnostics of diabetes is given in Table 2.1. Diagnostic indications for T1D includes polyphagia, polydipsia and polyuria [13].

Although there is not a definite cause of T1D, environmental and genetic factors precipitate the development of the disease. For instance, birth month and seasons are considered to have an impact on the incidence of T1D, as more people are diagnosed with diabetes in winter and fall [14], while people born in spring season have higher risk of developing T1D [15]. Additionally, T1D is a polygenic disorder and it was shown that the region HLA on chromosome 6 provides a tendency towards the chance of T1D development [16]. Ultimately, the process leading to the T1D occurrence is still unclear and fundamental questions about the underlying mechanism remains unanswered.

For the past decades, incidence of T1D has been raising worldwide. According to American Diabetes Association, 5-10% of diabetes patients have T1D [1]. In many European countries the amount of Type 1 diabetic people increases by approximately 3% annually [17-19]. The management of this disease and treatment for its secondary complications generates not only an economic but also a social burden to both researchers and patients. Hence, preventing or curing the disease is of utmost importance for many researchers in the field.

## **2.2 Current Treatment Strategies for T1D**

Although there is no cure for T1D [20], several strategies are employed to enhance patients' life quality by adjusting blood glucose levels to normal range. Among these strategies, insulin therapy is the most common and available treatment option. Other options include pancreas transplantation and islet transplantation. Pre-clinical and clinical studies also focus on tissue engineering approaches for immunoisolation of islets using scaffolds or different cell types (**Figure 2.1**).

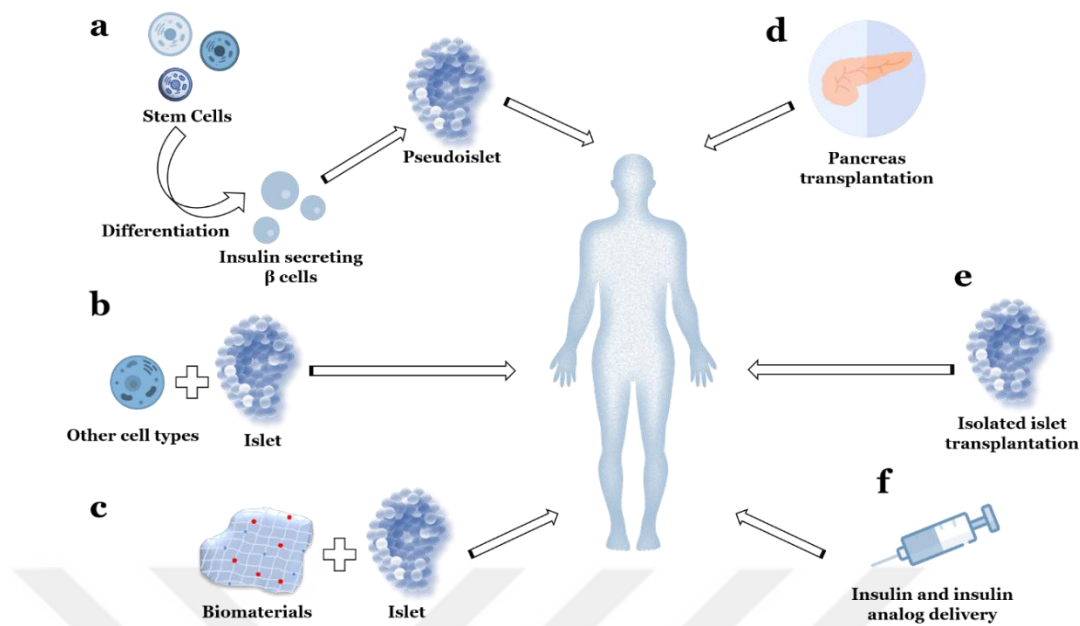


**Figure 2. 1.** Treatment strategies for T1D. (a) islets derived from stem cell differentiation. (b) co-transplantation or co-culture of islets/beta cells with other cell types. (c) islet transplantation with biomaterials such as hydrogel scaffolds. (d) pancreas transplantation. (e) isolated islet transplantation. (f) insulin therapy.

### 2.2.1. Insulin Therapy

Insulin is a protein with 86 amino acids and 6000 Da molecular weight. Today, insulin and its analogs are the only medicine options for the control of blood glucose levels in Type 1 diabetic patients [21]. The most common application of insulin therapy is achieved via multiple daily insulin injections. Along with the injections, insulin pumps are alternative treatment options. Blood glucose levels can be measured by a glucose biosensor simultaneously and an appropriate amount of insulin can be delivered to patient's bloodstream through a catheter that is placed subcutaneously. To overcome issues related with exogenous insulin activity, long-lasting insulin analogs are developed and these can also be used as alternative medication [22]. Although metabolic control can be achieved by insulin injections, they have severe side effects such as hypoglycemia, skin infections and weight gain [23].

### 2.2.2. Pancreas Transplantation

With the transplantation of pancreas, the aim is to eliminate the need for exogenous insulin and achieve normoglycemia [24]. Worldwide, 29,962 patients received vascularized pancreas transplantation between 1988 and 2016, according

to United Network for Organ Sharing statistics [25]. Although patients attain normal blood glucose levels after a successful operation, they require lifelong use of immunosuppressive drugs. Additionally, daily usage of immunosuppressive drugs causes severe side effects, even leading to kidney failure. In addition, donor shortage and the risk of whole organ operation are other limitations to wider application of this strategy [3].

### **2.2.3. Islet Transplantation**

Islets of Langerhans can be described as islands of  $\beta$  cells surrounded by pancreatic exocrine tissue [26]. Islets comprise approximately 2-3% of pancreas volume and they require a large portion of blood flow to pancreas [2]. Islet transplantation is an emerging option for T1D. It has advantages over pancreas transplantation, such as not requiring a major surgery, minimized immunosuppression, and a lesser extent of economic burden [4].

For the first time in 1972, islet transplantation reversed diabetes in a rodent model by Lacy group [27]. In 1989, the first clinical trial was achieved by the same group, where they could reverse T1D in a human patient, using human islets [28]. Although there have been hundreds of successful islet transplantation surgeries and patients who attained normoglycemia for the following years, islet transplantation still has many limitations. For example, during the islet isolation process which contains collagenase-digestion of pancreas from cadaveric donors, crucial extracellular matrix (ECM) components are lost. The loss of ECM components may cause a cutback in islet function and poses a problem against vascularization [11]. Additionally, the site of islet transplant has a critical effect on islet survival and function and the optimal implantation site is yet to be determined for human patients. Donor shortage is another issue, where generally islets of 2-4 cadaveric donors are required to cure 1 patient [29]. After islet transplantation, grafts need blood supply to remain viable and functional, hence vascularization around islets is critical which is not optimized in the clinical setting. Last but not least, immune reactions against islet grafts necessitates the use of immunosuppressive drugs [24]. Therefore, many groups from biomedical and tissue engineering fields have focused on immunoisolation, vascularization and functional improvement of islets.

## 2.3 Islet Engineering

To overcome limitations of islet transplantation mentioned in the previous section, engineering of islets can be done by mimicking naïve islets. Islet engineering deals with formation of islet-like organoids, or pseudoislets, improving islet function and survival by co-culturing  $\beta$  cells with specific cell types and immunoisolation and vascularization of pseudoislets with the help of functional biomaterials.

### 2.3.1. Formation of $\beta$ Cell Organoids

Reconstitution of pancreatic islets *in vitro* is another approach for islet therapy. The term “organoid” stands for a tiny and simplified version of an organ that functions in a very similar manner as its analogous. The ideal way to form  $\beta$  cell organoids is to use induced pluripotent stem cells (iPSC) and differentiate them into  $\beta$  cells [30]. This concept is ideal since it can overcome donor shortage and immune-related drawbacks by utilizing cell source from patients. However, at present, full differentiation of stem cells into  $\beta$  cells is not achieved. Therefore, numerous tissue engineering strategies are exploited to fabricate islet-like organoids from different cell sources.

Various rodent cell lines that have the ability to secrete insulin in response to glucose are being used for research. In this approach, different  $\beta$  cell lines are cultured in a 3D environment to induce the formation of islet-like spheroids. Rat insulinoma 5 (RINm5F), mouse insulinoma 6 (MIN6), INS-1,  $\beta$ TC6 cell lines are some examples for insulin secreting cell lines that can be used to form  $\beta$  cell organoids [31].

Architecture of  $\beta$  cell organoids is critical for their function and viability. The spheroid structure of native islets must be mimicked for pseudoislet formation, since cell-to-cell contact is essential for signaling, hence insulin-secretion. It was reported that beta cell spheroids were more functional than monolayer grown cells [32].

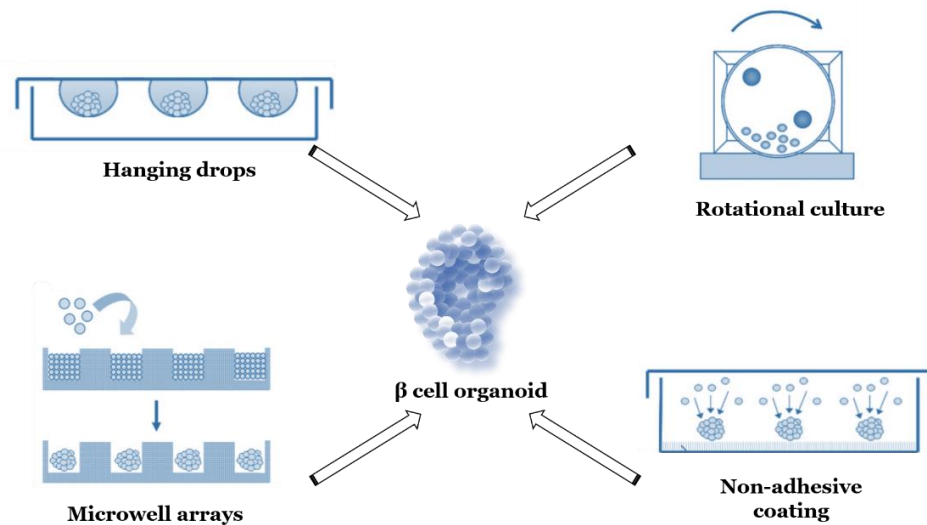


**Figure 2. 2.** Methods for  $\beta$  cell organoid formation

There is a variety of methods to form beta cell organoids (**Figure 2.2**). The object of these methods is to generate spherical-shaped, homogeneous, functional and viable organoids that can serve as replacements of native islets in islet therapy for T1D.

For example, beta cell organoids can be formed by self-assembly, either in static or dynamic conditions. In self-assembly methods, cells are cultured in custom design or common tissue culture flasks and cell aggregates are formed. For example, single  $\beta$  cells can form aggregates dynamically by spinning at a certain rate after a particular amount of incubating period. The type of tissue culture plate is important, therefore usually non-adhesive plates or rotational cell culture systems (RCCS) are used [33].

Microwells are also useful tools to form uniform shaped and large numbers of  $\beta$  cell spheroids. In this method, wells have depths and diameters in the range of tens to several hundred micrometers. Cells that are seeded on microwells settle down by gravitational forces and a spheroid is formed in each well [34].

Another well-known method for  $\beta$  cell spheroid formation is hanging drops. In this 3D culture technique, cell suspensions are placed onto the lid of tissue culture dish. Next, the lid is inverted, and droplets are kept in place due to surface tension. After a certain amount of incubation, as a result of gravity, cells accumulate and aggregate into spheroids. This technique is convenient for mimicking native islets by using  $\beta$  cells since the aggregates have neat spherical shapes and their sizes are

homogeneous. Droplet volume is between 20-50  $\mu\text{l}$  and cell number within the droplet can be changed between 200-15000 cells. Diameter of the spheroid depends on both cell number and droplet volume and it can be between 100-1200  $\mu\text{m}$  [33, 35, 36].

### **2.3.2. Prevention of Islet Graft Failure**

After the initial success of islet transplantation in human patients [37], with the development in islet isolation and maintenance, clinical islet transplantation outcomes continued to improve [38, 39]. However, after the implantation, islet graft is recognized as foreign by host body, leading to immune attacks to the graft. To suppress this effect and prevent graft failure, immunosuppression is mandatory. However, the necessity of immunosuppressive drug administration after transplantation hinders insulin secretion ability of grafts even when drug doses are fairly low [40]. Also, using immunosuppressive medication, including rapamycin-based drugs, may bring about severe complications such as hyperlipidemia, mouth ulcers, hypertension and kidney failure [41]. Therefore, instead of using immunosuppression, immunoisolation of islets prior to transplantation is suggested. The main goal of immunoisolation of islets is to form a barrier between graft and host body, so that immune cells, namely leukocytes, macrophages and dendritic cells, would no longer recognize the graft as foreign [42]. Strategies regarding to immunoisolation of islets can be divided as cell-based and material-based approaches.

#### **2.3.2.1. Cell-based Methods**

Cell-based strategies to overcome islet graft rejection include co-culturing  $\beta$  cells with different cell types and forming a “heterospheroid”, a multicellular organoid. Other methods are surrounding islets with cells or co-transplantation of islets and other cells. In addition, regulating immune system via immune cell or ligand incorporation is an interesting and promising approach for preventing islet rejection in T1D treatment.

The key role of other cell types that are used as accessories to  $\beta$  cells is their regulatory function on immune cells. In many *in vivo* studies, normoglycemia was achieved by co-transplantation of intact mouse islets with other cells [9, 43]. For instance, islets co-transplanted with B6 mouse hepatic stellate cells (HSCs) demonstrated significantly improved graft survival [44]. Another example is

mesenchymal stem cells (MSC), which are widely investigated in co-culture studies owing to their regulatory role on immune system. MSCs secrete factors such as transforming growth factor- $\beta$  (TGF- $\beta$ ), hepatocyte growth factor (HGF) and indoleamine 2,3-dioxygenase (IDO) which contribute to cell to cell interactions for immune cells [45]. Additionally, (pre)adipocytes [46], microalgal cells [47], pancreatic  $\alpha$  cells [48], chondrocytes [49, 50], endothelial cells [51-57] and Sertoli cells [10, 58] have been investigated for co-culture studies.

Another cell type that has immunoregulatory activity is stellate cells (SC). As the name suggests, stellate cells are star-shaped cells that are majorly present in liver (hepatic stellate cells, HSC) and pancreas (Pancreatic stellate cells, PSC). Both HSCs and PSCs can synthesize ECM components such as collagen [59, 60].

HSCs have the ability to expand Treg population and suppress the actions of T cells. In recent studies, co-transplantation of HSCs with islets demonstrated that the presence of HSCs improved islet acceptance by protecting the graft from immune attack *in vivo* [61-65]. SCs can also stimulate vascularization by secreting proangiogenic factors such as VEGF [66]. Since vascularization plays a key role delaying/preventing graft rejection, this ability is perceived as a great advantage. For example, Yin et al. co-transplanted HSCs with islets *in vivo*, and have observed higher extent of angiogenesis around islet grafts, which promoted islet acceptance in BALB/c mice [67]. SCs form fully biocompatible barriers around islets and hold great potential for both immunosuppression and angiogenesis aspects of islet graft survival.

### **Regulatory T cells (Tregs)**

Regulatory T cells are immune cells that have a regulating or suppressing function over other immune cells such as effector T cells. There are two types of Tregs: natural Tregs (nTregs), which are produced by thymus and adaptive Tregs (aTregs), which are produced by differentiation of Tregs outside thymus [68]. nTregs express CD4 and CD25 receptors. They are also characterized by Forkhead box P3 (FoxP3) transcription factor, which determines the development and function of Tregs [69].

Tregs produce cytokines such as interleukin 10 (IL10) and transforming growth factor beta (TGF $\beta$ ), which have immunosuppressive properties. They are

generally recruited through ligand-receptor interactions. Receptors that are present on the Treg cell membrane (such as IL2) can bind ligands like antigens, cytokines or chemokines. Tregs also have a significant role in cancer immunology. It was demonstrated that most cancerous cells can recruit Tregs and circumvent immune system. Therefore, not being recognized, cancer cells can keep growing without receiving any immune response from the body [70].

Tregs mediate the immune system by diminishing T cell activity, therefore, they are promising for the treatment of autoimmune diseases such as T1D [71]. In a study, Treg recruitment to islet graft was accomplished by Fas-ligand interactions and graft acceptance was enhanced [72]. To summarize, Tregs can be considered as tools for creating an immunological barrier for islet grafts.

### **Chemokines**

C-C motif ligand 22 (CCL22) is a ligand of recently found chemokine CCR4 [73]. Studies demonstrated that cancer cells can secrete CCL22 to recruit Tregs to tumorous tissue. Tregs are recruited to the area via CCR4 receptor-CCL22 ligand interaction and restrain effector T cell actions, thereby silencing the immunological attacks [70].

Based upon findings of cancer immunotherapy, the role of CCL22 in manipulating immunological processes has been studied and exploited in other areas too, such as for T1D diabetes treatment. For example, pancreatic islets expressing CCL22 showed not only Treg recruitment but also graft tolerance [74, 75]. Therefore, CCL22 chemokine holds a great promise for the immunotherapy approach for T1D treatment.

### **2.3.2.2. Material-based Methods**

Coating or encapsulating islets with biomaterials is another widely explored approach for immunoisolation [76]. In these strategies the main idea is to form a barrier between islets and implantation site which allows the exchange of oxygen and nutrients, removal of waste and block the entrance of immune cells (**Figure 2.3**).

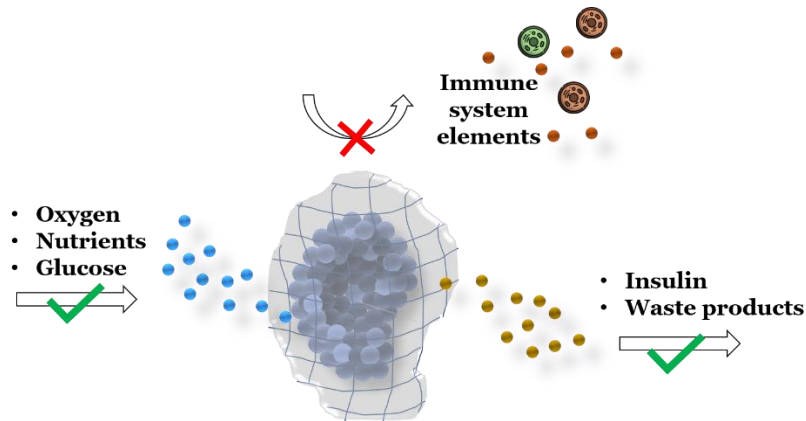


**Figure 2. 3.** Immunoisolation of islets with biomaterials

Biomaterial selection is essential in this case. They should be fully biocompatible and should not require harsh chemistries that might danger the integrity of islets. Natural and synthetic semi-permeable biopolymers are extensively used to form an immunoisolation barrier around islets.

### **Materials for Islet Coating**

Biocompatible materials with easily modifiable characteristics have been extensively investigated and considered as scaffolds for immunoisolation of islets. The most commonly employed materials for islet coating are alginate [77], agarose [78], chitosan [79], collagen [80], and polyethylene glycol (PEG) [81] (**Figure 2.4**).

Among these materials, alginate is by far the most frequently exploited biomaterial. Alginate is a natural polymer found in brown seaweeds and bacterium. They are polysaccharides with mannuronic and guluronic acid chain units [82]. Alginate gets crosslinked under mild conditions such as physiological pH and temperature in presence of calcium ions [83]. Since crude alginate contains endotoxins and polyphenols, which are toxic to cells, the purification of alginate is an essential step towards obtaining a biocompatible material [84]. Alginate was used for the first time in 1980 to encapsulate approximately 3000 islet equivalents (IEQ) for an in vivo study conducted with streptozotocin (STZ)-diabetic rats. In the study, diabetes could be reversed for 21 days after implantation while naked islets could reverse diabetes only for 8 days [77]. In 1994, alginate-encapsulated islets were used to treat the first human patient suffering from T1D. The patient attained normoglycemia for 9 months, without any exogeneous insulin treatment [85]. Following years, many clinical trials were made, and successful results were

obtained [86-89]. Although there have been many promising clinical accomplishments, most alginate-encapsulated islet recipients return to hyperglycemia and require insulin injections, not to mention life-long immunosuppression [89].

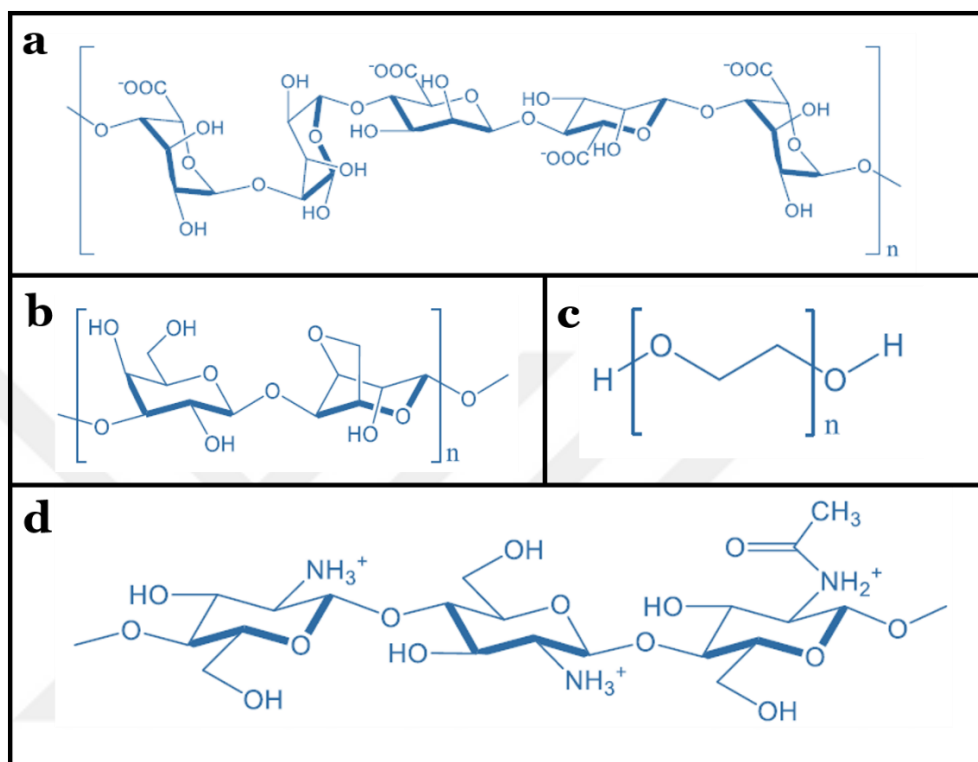


**Figure 2. 4.** Chemical structures of the most commonly used polymers as immunoprotective barriers for islet transplantation. (a) alginate. (b) agarose. (c) poly(ethylene glycol) (PEG). (d) chitosan.

Agarose is another natural polymer and just as alginate, it is obtained from seaweed. This polysaccharide can form gels that is thermally reversible [90]. By reducing the temperature, agarose microbeads can be form in the presence of islets. In an *in vivo* model, islets were encapsulated in agarose beads and normoglycemia was achieved post transplantation [91]. The major drawback of agarose might be the cellular diffusion through the gel membrane [90].

Chitosan is a polysaccharide that is obtained by deacetylation of chitin, which is found abundantly in insects. Chitosan can go into gelation ionically or chemically and it is a biodegradable and biocompatible polymer. It has amino and hydroxyl groups which can be substituted with functional moieties [92]. Chitosan was used as an immunological barrier, where chitosan-encapsulated islets were

transplanted to mice and reversal of diabetes was observed [93]. Since chitosan is not water soluble in physiological pH, its biomedical applications are limited and only feasible after PEGylation.

Poly (ethylene glycol) (PEG) is a water-soluble and synthetic polymer. It is extensively used in tissue engineering [94, 95], drug/gene delivery [96-98] and biomedical applications due to its high biocompatibility and versatility [99]. PEG is completely inert, hydrophilic and easily modifiable with functional groups which makes them superior to other biopolymers [100, 101]. A derivative of PEG, poly (ethylene glycol) diacrylate (PEGDA), is a photopolymerizable version of PEG that is investigated widely as immunoisolating barriers for islet transplantation. PEGDA can be crosslinked in the presence of a photoinitiator with a laser source to yield hydrogels. In tissue engineering applications semipermeable PEG hydrogels are considered as great materials for islet coating not only because their processing can be made in aqueous environments at physiological pH but also, they can be functionalized with biological cues such as peptides, growth factors and lipids to mimic the nature of ECM. For example, cell adhesion ligand and GLP-1 modified PEG hydrogels were used to encapsulate islets with MSCs [95]. In the study, addition of these peptides to PEG hydrogel increased insulin release in high glucose buffer, hence increasing the stimulation index. Teramura and Iwata used biotinylated PEG-lipid to coat islets conformally [102]. With their approach, they managed to encapsulate islets with a thin layer of PEG, which minimized the issues about molecular transport through membrane while preventing instant blood-mediated inflammatory responses (IBMIR).

### **Strategies for Islet Coating**

Coating or encapsulating islets within semi-permeable materials can be done in several ways, such as macro- and microencapsulation and conformal coating (i.e. layer by layer technique) (**Figure 2.5**).

Macroencapsulation is simply encapsulating multiple islets within a capsule that has dimensions  $>1\text{mm}$ . Intravascular devices are connected to patients vasculature, therefore nutrient and oxygen diffusion is enhanced while the protective membrane works as immunoisolator [103]. Although there are many

successful animal studies, problems associated with IBMIR prevents FDA to approve these microencapsulation devices for clinical trials [104].

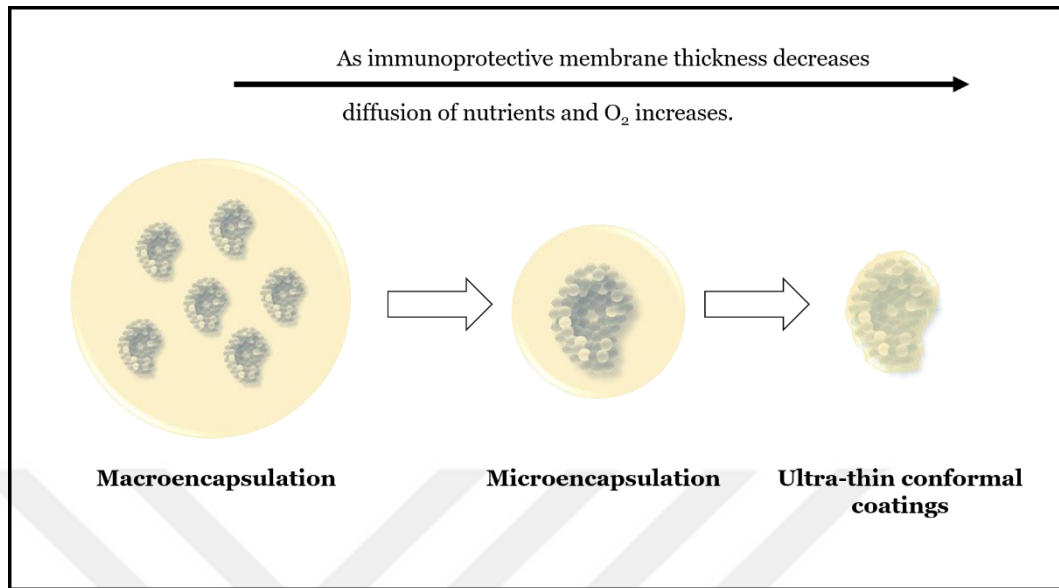


**Figure 2. 5.** Islet coating strategies

Compared to microencapsulation, microencapsulation offers thinner membranes around islets, which is desirable since a higher rate of nutrient and oxygen diffusion can be achieved with thin coatings. Due to their spherical shapes, microcapsules have high surface area/volume ratio, which also contributes to molecular transport through the membrane. There are numerous pre-clinical studies conducted with animals and phase I trials with humans using this strategy [86, 105-107]. Alginate microcapsules are widely used for in vivo studies and they have been used for clinical human trials. Humans receiving purified alginate encapsulated islets did not create any immune response while attaining normoglycemia [108].

Conformal coatings forms nano-thin layers around islets. This nano-thin membrane contributes to islet survival by decreasing diffusion distance between islets and graft site. In addition, by minimizing the coating thickness, transplant volume is also reduced which allows a less invasive surgeries by portal vein infusion [104]. The most extensively used polymer for conformal coatings is PEG. For example, by using functional PEG derivatives, layers of PEG films can be deposited onto islets. In a study, maleimide-PEG-lipid was deposited on islets, next PEG-thiol and PEG-maleimide micelles were deposited one-by-one to obtain a membrane with thickness of tens of micrometers [109]. By using the hydrophobic

interactions between cell membrane and lipid and then using the well-known maleimide-thiol reaction, a stable membrane was fabricated. It was shown that these membranes did not hinder the insulin secretion function of encapsulated islets while reducing IBMIR when they are exposed to human whole blood and serum [109]. In another layer-by-layer study, islets were coated with PEG layers through biotin-streptavidin interactions [110]. The outer layer of the membrane included glucose like peptide (GLP-1), which plays a key role in glucose metabolism. It was shown that the coating improved insulin secretion and islet viability was conserved. It is also possible to combine material- and cell-based approaches to create a superior immunoisolation. For instance, Teramura et al. deposited PEG layers via lipid-cell membrane hydrophobic interactions by using biotin-PEG-lipid [111]. Next, they used streptavidin-immobilized HEK293 cells to attach these cells to islet surface. They showed that insulin secretion ability and viability of islets were maintained after cell immobilization on islets.

#### 2.4 Water-in-water (W/W) Emulsions

W/W emulsions, also known as aqueous two-phase systems (ATPS), are colloidal dispersions of two phases that are immiscible [112]. W/W emulsions consist of a “dispersed phase” and a “continuous phase”, where droplets of one aqueous solution is distributed in the other (**Figure 2.6**). Phase separation in W/W systems is rapid, usually two distinct phases are formed within seconds. However, the colloidal stability of these emulsions is weak since the repulsion forces between droplets are deficient. Therefore, unless any stabilization agent is added, W/W emulsions are very unstable.

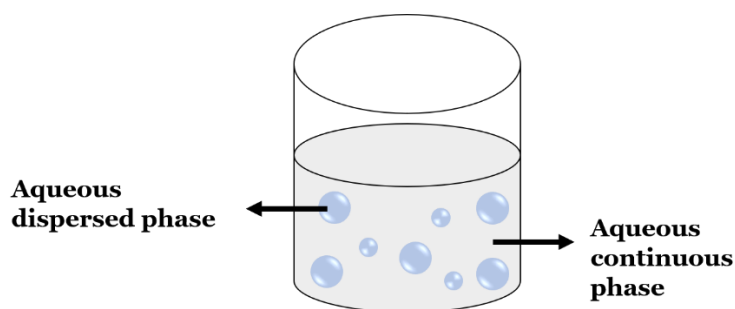


**Figure 2. 6.** Schematics for W/W emulsions

#### **2.4.1. Preparation and Stabilization of W/W Emulsions**

W/W emulsions can be prepared by applying a mechanical mixing force to the system. In these aqueous two-phase systems, when one solution is added to the other, a phase separation occurs. Next, applying a mechanical force, one phase that has a smaller volume fraction gets dispersed inside the other phase. For this purpose, simple stirring, vortexing, ultrasonication, and shaking can be used.

The major drawback of W/W emulsion is their unstable nature. Especially when both phases are near their critical points, droplets tend to coalesce, and phases separate irreversibly. To stabilize these systems, many techniques have been developed. For instance, emulsions can be stabilized by adding particles to the systems, such as latex or silica particles [113]. In this approach, particles adsorb on the interface, preventing aqueous droplets from colliding with each other. Stabilization can also be obtained by using globular proteins. In that case, protein particles are initially heated up to control their morphology and surface properties. Preheating determines the surface charge of particles, which also determines the affinity of particles to either phase. Next, they are added to ATPS, and depending on the pH value of the solutions, they get positive and negative charges and prefer which phase to adsorb on, thereby stabilizing the emulsion [114]. Pickering emulsions are another option to prepare a stable W/W emulsion. Solutions of PEG and dextran were mixed together with microparticles of acrylate and methacrylic acid and particle adsorption was observed at pH 7 to 7.5 [115]. This study demonstrates that depending on pH, stabilization and destabilization of emulsions can be achieved.

Droplet sizes in dispersed phase can be controlled by tuning the agitation characteristics. For example, in a maltodextrin-gelatin ATPS, droplet size was controlled by adjusting the shear rate applied to the system [116]. It was shown that droplet size increased at slower shear rate values. In another study, size of photopolymerized PEG hydrogel particles in PEG/dextran ATPS were tuned by altering the power and exposure of laser [99].

#### **2.4.2. Applications of W/W Emulsions**

W/W emulsions are effective systems for the extraction and separation of macromolecules from biological mixtures. For instance, lipase, the enzyme that catalyzes fat hydrolysis, can be extracted and purified by PEG/phosphate W/W

emulsion system [117]. ATPS also hold great potential in food industry, as emulsions made of gelatin and different polysaccharides are considered in several food formulations [118]. To protect the active ingredients of foods and to adjust the digestion rate, W/W emulsions can be employed [119]. Synthesis of microgel particles through W/W emulsions is an extensively studied application of ATPS. These microgels have a variety of applications such as drug/gene delivery[97, 99] and diagnostic agents [120].

#### **2.4.3. PEG Hydrogel Particles**

W/W emulsions are widely used for the synthesis of PEG-based hydrogel particles. Once an aqueous PEG phase is dispersed in a continuous phase, droplets can be crosslinked chemically, thermally or optically to yield in microgel particles. For example, Franssen and Hennink prepared PEG microgels by W/W emulsion technique [121]. They used dextran, magnesium sulfate, poly (vinyl pyrrolidone) and Pluronic F68 as continuous phase and compared the diameter and morphology of PEG particles prepared in these different experiment groups. PEG/dextran emulsion system was studied extensively by altering PEG and dextran phase concentrations and the system was stabilized using triblock copolymers [122]. Peptide functionalized PEG hydrogel microspheres were synthesized by Murphy et al.[123-127]. VEGF release from microgels and angiogenesis was studied *in vitro* and *in vivo*. PEG/dextran system was used to prepare PEG particles with matrix-metalloproteinase (MMP)-sensitive and RGDS peptides. Hydrogel particles were prepared by photopolymerization of PEGDA after emulsion process, loaded with QC drug and apoptotic activity was investigated. Drug-loaded, biodegradable and peptide-functionalized microgels for cancer therapy could be prepared by W/W emulsion system [94].

Chapter 3  
**Recruitment of Regulatory T Cells to Implant Site in Islet Transplantation by Beta-Stellate Cell Organoids**

**3.1. Introduction**

T1D is an autoimmune disease caused by  $\beta$  cell destruction in pancreas. Consequently, people suffering from T1D cannot produce the insulin they need for glucose metabolism [12]. Therefore, type 1 diabetic patients have high blood glucose levels while their cells are deprived from metabolic fuel.

Insulin treatment is the most commonly used strategy to overcome problems associated with T1D. However, this treatment is not aimed to reverse diabetes, it only adjusts blood glucose levels of patients to minimize the symptoms of the disease. Another option is pancreas transplantation. Although after successful operation patients regain their ability to secrete insulin and achieve normoglycemia, they are required to use lifelong immunosuppressive drugs. In addition, pancreas transplantation is a risky operation where patients with end-stage diabetes also receive a kidney transplant as well [128]. Donor shortage is another factor limiting the whole organ transplantation. Islets are the vital compartments of pancreas and they are clusters of insulin-secreting  $\beta$  cells. Compared to pancreas transplantation, islet transplantation is a minimally-invasive approach and holds great potential in clinical studies. However, after islet transplantation, immune-system still needs to be suppressed. Additionally, multiple cadaveric human donors are required to treat one diabetic patient, meaning that donor shortage is still an issue [129].

To lessen post-operation immunosuppression requirements, several strategies, including material-based and cell-based, have been considered for islet therapy. When islets from donors are implanted, the immune system of the patient recognize the implant as a foreign body, therefore immediately attacks to destroy the islets. The main idea of material-based strategies is to create a protective barrier between islets and the environment which lets oxygen and nutrients in and blocks immune system components at the same time. Several clinical studies on humans

with biomaterial-encapsulated islets were conducted. For example, 4 patients receiving alginate-encapsulated islets attained normal blood glucose levels, however, they still had to use immunosuppressive drugs [108]. Cell-based immunotherapeutic strategies have also been used to prevent islet destruction. In this approach, islets are co-transplanted with companion cells, such as MSC and endothelial cells. Companion cells must have a regulatory function on the immune system, where they silence the actions of lymphocytes and macrophages and protect islet implant from being destructed [43, 70].

Pancreatic and hepatic stellate cells (PSC and HSC) have immunomodulatory activities, where T cell activities can be suppressed by HSCs, while regulatory T cells (Tregs) are expanded. *In vivo* studies with islets and HSCs showed that islet rejection could be prevented by co-transplantation [62, 65]. In addition to their immune system regulatory functions, HSCs can also promote vascularization by secreting VEGF [66, 130].

Cancer cells are body's own cells which are able to avoid immune reaction by secreting chemokines and recruiting Tregs. CCL22 is a chemokine secreted by cancer cells, and it recruits Tregs by binding CCR4 receptor found in Treg membrane [131]. Studies with CCL22 protein has confirmed that it is capable of providing an immune barrier by attracting Tregs and thereby protecting islet implants [74, 75].

In this chapter, we designed an *in vivo* study with diabetic mice. A multicellular organoid was fabricated, in which insulin-secreting  $\beta$  cells and CCL22-expressing HSCs were co-cultured using hanging drop technique. By combining intrinsic immunomodulatory characteristics of HSCs with Treg recruitment capability of CCL22 protein, we have engineered a superior  $\beta$  cell organoid which overcomes issues related with immunosuppression. These multicellular organoids were transplanted to STZ-induced diabetic mice and Treg recruitment was observed around implanted grafts. This approach is promising not only for the treatment of T1D but also for many other cell delivery therapies where attacks from immune system is required to be suppressed.

## **3.2 Experimental**

### **3.2.1 Cell Culture**

Human HSCs were provided from Koç University Hospital. HSCs were cultured in DMEM:F12 medium (Gibco) supplemented with 10 % fetal bovine serum (FBS) (heat inactivated, Gibco) and 1% Penicillin Streptomycin (Sigma) and incubated at 37°C with 5% CO<sub>2</sub>. β-TC-6 cells were obtained from ATCC and cultured in high glucose DMEM medium (Gibco) supplemented with 10% FBS, 1% L-Glutamine (Sigma), 1% sodium pyruvate (Lonza), and 1% Penicillin Streptomycin (Sigma) and incubated at 37°C with 5% CO<sub>2</sub>. HEK293T cells were provided from Dr. Tugba Balci Onder from Koç University. HEK293T cells (up to passage 10) were cultured in DMEM (Gibco) with %10 FBS, and %1 Penicillin Streptomycin and incubated at 37°C, and %5 CO<sub>2</sub>.

### **3.2.2 Plasmid constructs**

For PCR-based cloning, pCMV6-AC including the CCL22 gene was used as template. Primers for PCR were designed to add BamHI and SalI restriction enzyme recognition sites on either end of the gene. CCL22 amplification was done by PCR. To remove unwanted salt, enzyme and nucleotides, products of PCR were purified by using Macherey Nagel NucleoSpin® Gel and PCR Clean-up kits. Next, they were digested with BamHI and SalI to acquire restriction enzyme recognition site at the ends of gene. Retroviral vector pBABE was also digested with both BamHI and SalI to linearize and then dephosphorylated by Antarctic Phosphatase to prevent self-ligation. Insert, and recipient vector were run on 1% agarose gel and extracted from via Macherey Nagel NucleoSpin® Gel and PCR Clean-up kit. Next, CCL22 insert was ligated to recipient retroviral vector pBABE by T4 DNA ligase overnight at 16°C. Next, ligated plasmid was transformed into One Shot™ Stbl3™ chemically competent cells and then injected to agar plate with ampicillin. After 16 hours of incubating, colonies were picked and injected to LB Broth medium with ampicillin and incubated for 16 hours. Plasmid DNA was isolated from the bacteria culture by using Macherey Nagel NucleoSpin® Plasmid kit.

### 3.2.3 Virus Production and Infection of Hepatic Stellate Cells

$2.5 \times 10^6$  HEK293T cells were cultured in 10 cm tissue culture dish and incubated overnight. pBabe-GFP vector was used as control group in transduction experiments. pBabe-GFP or pBABE-CCL22 and viral packaging vectors pUMVC pCMV-VSV-G were used to transfect HEK293T cells via Fugene transfection reagent (Promega). Next day, culture medium was refreshed with new medium and incubated overnight at 37 °C and %5 CO<sub>2</sub>. Medium with virus particles was collected and stored at -80°C. Viruses were 100X concentrated by using % 50 (w/v) PEG solution. SCs were seeded in 6 cm tissue culture plates at a density of 120.000 cells/plate. Next day, cells were infected with GFP or CCL22 in the presence of 10 µg/ml protamine sulfate (PS) and incubated for 2 days at 37 °C and %5 CO<sub>2</sub>. To increase transduction efficiency, infection was done twice. SCs were chosen by adding puromycin to a final concentration of 1µg/ml for 3 days.

### 3.2.4 CCL22 Protein Determination

$12 \times 10^4$  transfected HSCs were seeded on 6 cm tissue culture dish and medium was changed after 2-3 days. Next, medium was collected 5 days after seeding and CCL22 protein levels in culture medium were analyzed by Human Quantikine CCL22 ELISA kit (R&D Systems) following the manufacturer's instructions.

### 3.2.5. Multicellular Organoid Formation by Hanging Drop Technique

Multicellular organoids composed of 1:1 β-TC-6:HSC-CCL22 cells were prepared by hanging drop method (**Figure 3.1**). β-TC-6 cells and transfected HSCs were grown in 6 cm tissue culture dishes. At 80-90% confluency, cells were detached from the dishes by trypsinization. Cells were counted under hemocytometer and cell density was adjusted to 300 cell/30µl medium. Hanging drop medium consisted of β-TC-6 (50% (v/v)) and HSC (50% (v/v)) medium. A droplet of 30 µl contained a total of 300 cells: 150 β-TC-6 and 150 HSC-CCL22. 30 µl droplets of cell suspensions were pipetted onto the lids of 10 cm culture dishes. Next, the lids were gently inverted back to plates containing 8 mL PBS and 80µL penicillin streptomycin (PS). Hanging drops were incubated for 3 days at 37°C and 5% CO<sub>2</sub>.

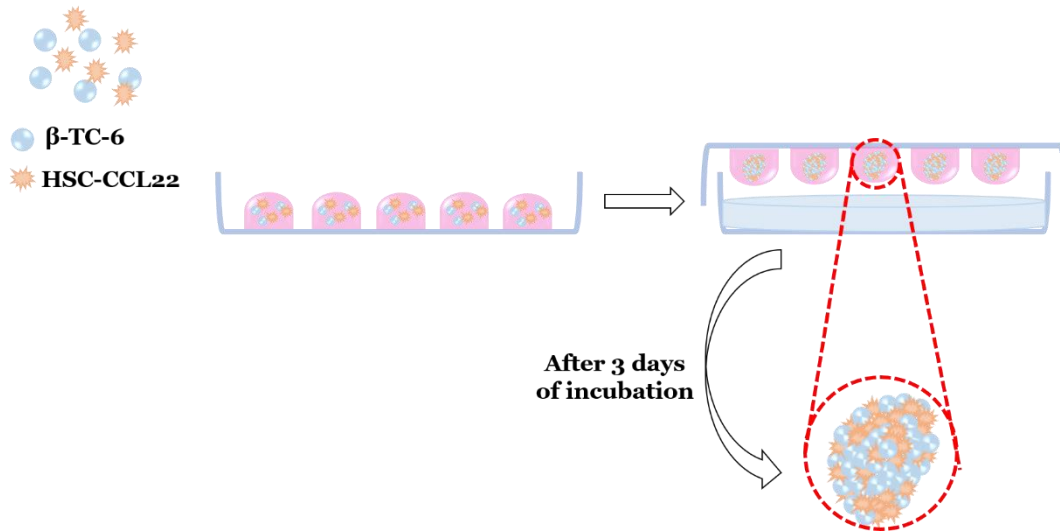


**Figure 3. 1.** Preparation of multicellular organoids by hanging drop method

### 3.2.6. Transplantation of Multicellular Organoids to Diabetic Mice

All *in vivo* experiments were approved by the institution review boards of Koc University (HADYEK). Diabetic male CD1 mice were used and maintained in conventional housing at the Animal Research Facility of Koç University (KUARF) for *in vivo* experiments. For diabetes induction, male CD1 mice weighing 28-33 g received intraperitoneal injection of streptozotocin (STZ) (AdipoGen) at a dose of 50 mg/kg body weight for five consecutive days. After STZ injection, animals were monitored for fasting blood glucose levels and weighted for seven days. Blood glucose was measured with Accu-Chek glucose meter from tail vein. Mice with a blood glucose level higher than 300 mg/dl were considered as diabetic and used for the transplantation experiments. 600  $\beta$ -TC-6:HSC-CCL22 multicellular organoids in 100 $\mu$ L PBS were implanted into left abdominal external oblique muscle of diabetic mice and maintained for 10 days. As control, only 100  $\mu$ L PBS was injected to left abdominal external oblique muscle of mice. Body weight of the transplanted mice was monitored at regular intervals. Tissues of same weight from both left abdominal external oblique muscle (implantation site) and right abdominal external oblique muscle (control) were surgically removed from mice 10 days after transplantation and analyzed by flow cytometer.

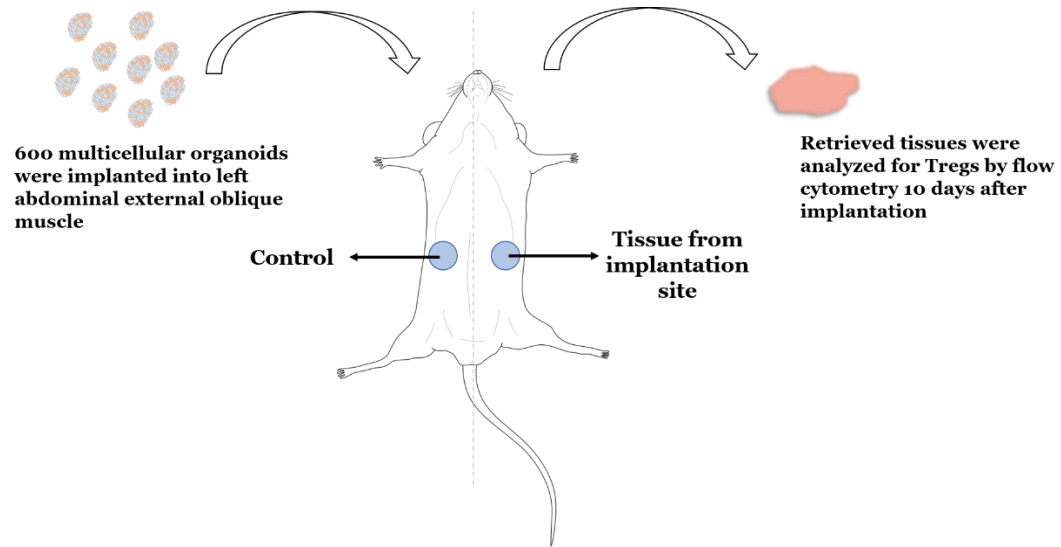


**Figure 3. 2.** 600 multicellular organoids were implanted to diabetic mice. Tissues were retrieved from animals at day 10 for flow cytometry analysis.

### 3.2.7 Flow Cytometry

Tissues from both implantation site and control site were retrieved 10 days after transplantation and analyzed for Treg recruitment. Briefly, Mechanical disrupting was applied first to isolate cells from tissue in serum free RPMI medium. Next, disrupted tissues were filtered through 70  $\mu\text{m}$  strainers to prevent aggregates. Cells were counted, and density was adjusted to 10000 cells/ $\mu\text{l}$ . True-Nuclear FoxP3 Mouse T-Reg Flow Kit (Biolegend) was used to detect CD4<sup>+</sup>FoxP3<sup>+</sup> Tregs in tissues. 20  $\mu\text{l}$  of Anti-Mouse CD4 APC/CD25 PE antibody cocktail and 100  $\mu\text{l}$  of sample were added to conical tubes, vortexed and incubated for 15 minutes in the dark at RT. Unstained sample tubes were used for autofluorescence detection for each sample. 2 ml staining buffer containing PBS with 0.5% (w/v) BSA was added and tubes were centrifuged at 400 g for 5 minutes. The supernatant was discarded, and cells were fixed and permeabilized with 1ml of 1X Transcription Factor Perm Buffer and centrifuged for 5 minutes at 400 g. Pellet was resuspended with 100  $\mu\text{l}$  1X Transcription Factor Perm Buffer. 5  $\mu\text{l}$  of Anti-Mouse FoxP3-Alexa488 antibody was added to the stained tubes and samples were incubated for 30 minutes in the dark at RT. Cells were washed twice with 2 ml 1X Transcription Factor Perm Buffer for 5 minutes at 400 g. Supernatant was discarded and pellet was resuspended with 500  $\mu\text{l}$  of staining buffer.  $10^6$  cells were analyzed with BD

Accuri C6 Flow Cytometer and using Accuri C6 Software (Becton Dickinson). CD25<sup>+</sup>FoxP3<sup>+</sup> cells under CD4<sup>+</sup> gate was determined as Tregs.

### 3.3. Results and Discussion

#### 3.3.1 Confirmation for CCL22 Transfection with ELISA Assay

To confirm the presence of CCL22 protein in transduced HSCs, human CCL22/MDC Quantikine ELISA assay was applied. As a control group, HSCs were transfected with GFP protein. High CCL22 concentrations ( $4117 \pm 387$  pg/mL) were observed for HSC-CCL22 groups, while no protein was detected from GFP-transfected group (**Figure 3.3**). This indicates the successful transfection of HSCs with CCL22 ligand.

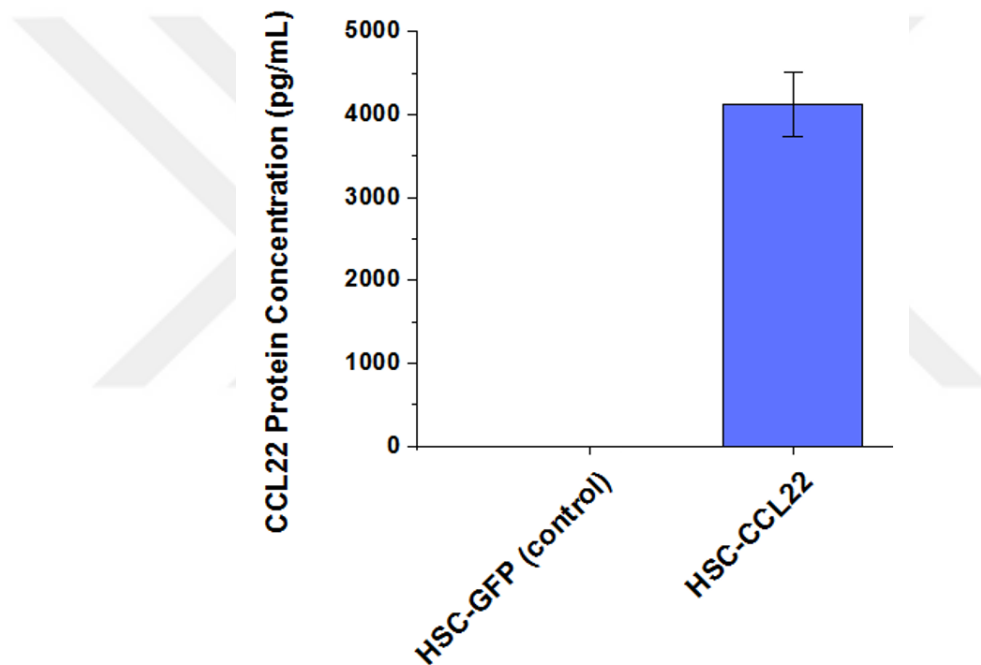


**Figure 3. 3.** Expression of CCL22 by transduced HSCs. Protein concentrations were quantified with CCL22 ELISA kit.

#### 3.3.2 Recruitment of Tregs in Diabetic Animal Model

600 multicellular organoids with 300 initial cell number and 1:1 cell ratio ( $\beta$ -TC-6 to HSC) were implanted to left abdominal external oblique muscle of STZ-diabetic male CD1<sup>+</sup> mice. For each animal, tissues from both left (implantation site) and right (control) abdominal external oblique muscle were retrieved 10 days after transplantation and assayed with True-Nuclear FoxP3 Mouse T-Reg Flow Kit.

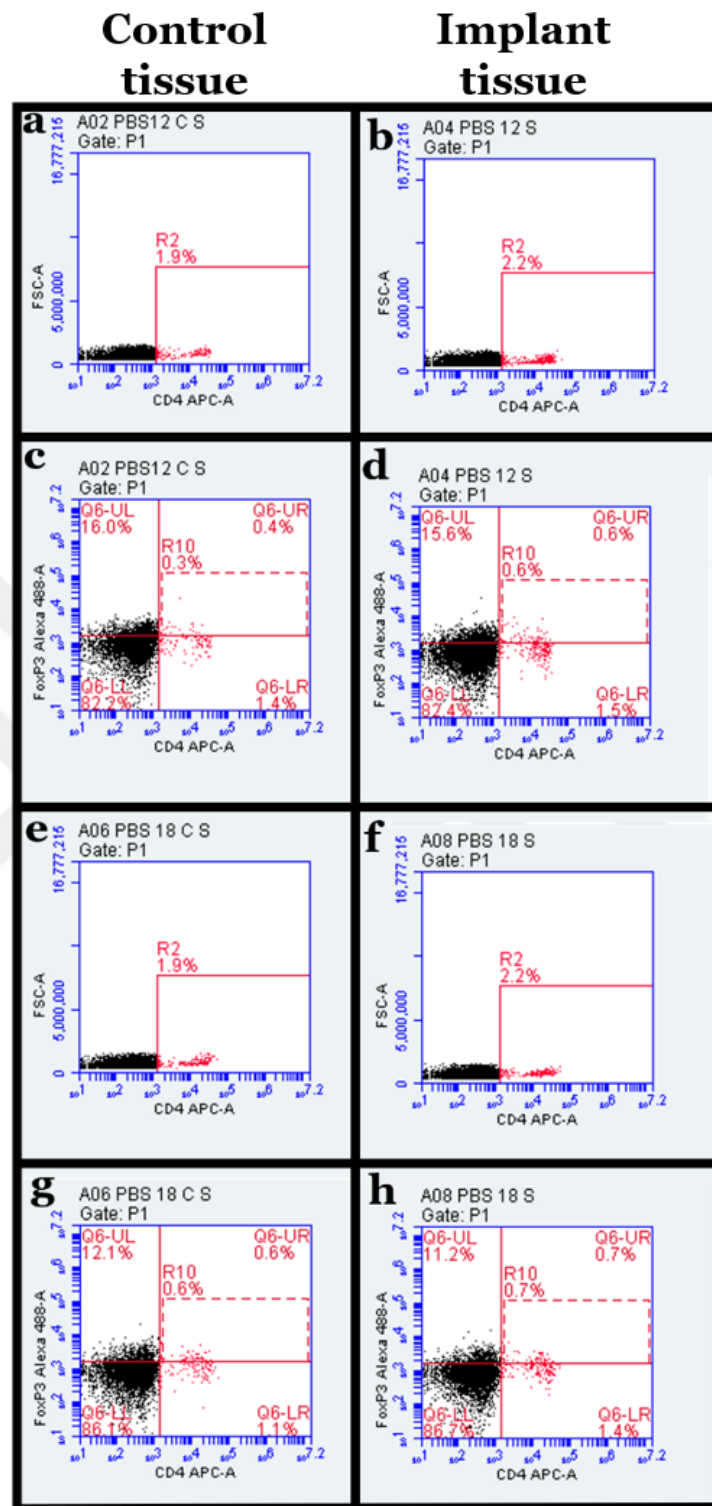


**Figure 3. 4.** Flow cytometry analysis results for PBS-treated control animals. 100 $\mu$ L PBS was injected into left abdominal external oblique muscle of STZ-induced diabetic mice. Tissues from implant site and a control site was retrieved 10 days after the procedure. Treg flow assay was performed to determine Treg recruitment by analyzing CD4+CD25+FoxP3+ cells. (a, c, e, g) Flow analysis results from control tissues and (b, d, e, f) Flow analysis results from implant tissue.

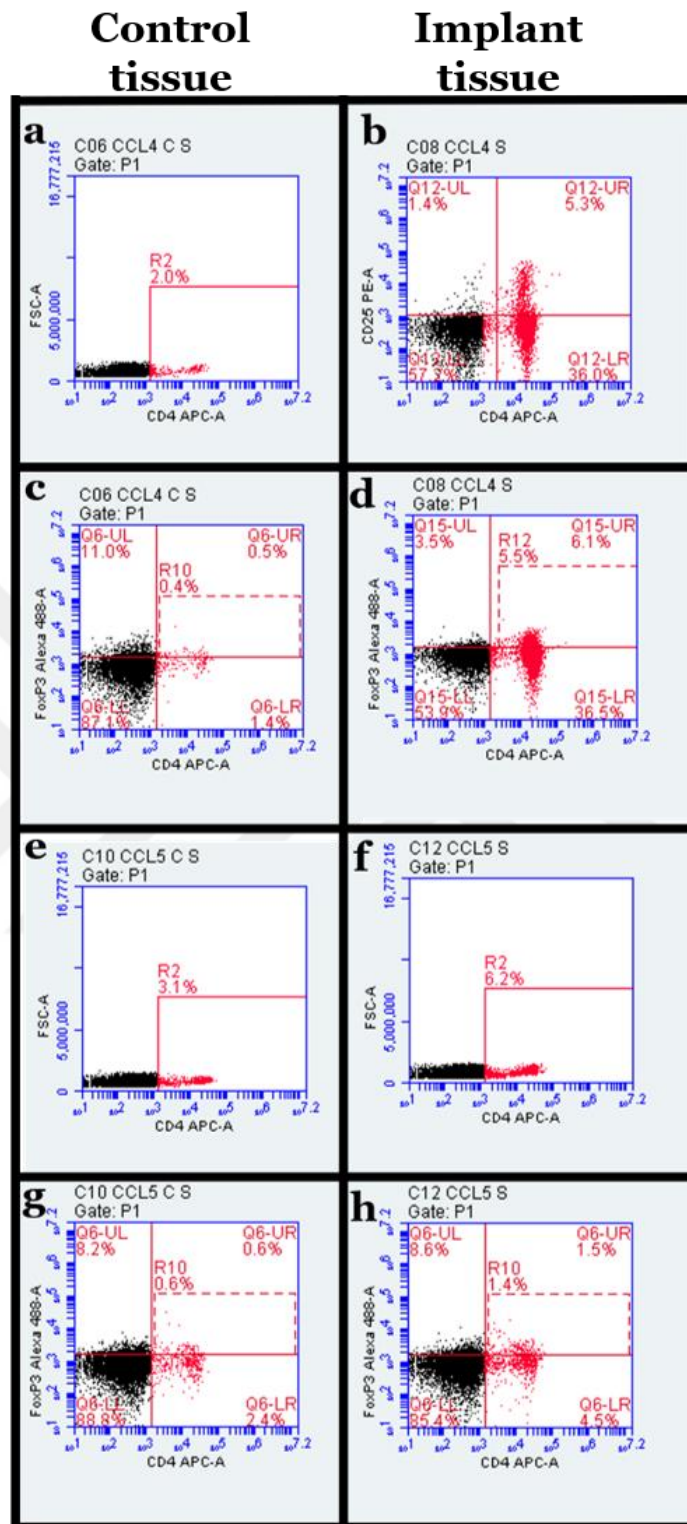


**Figure 3. 5.** Flow cytometry analysis results for organoid-implanted animals. 600 multicellular organoids of  $\beta$ -TC-6:HSC-CCL22 were implanted to STZ-induced diabetic mice. Tissues from implant site and a control site was retrieved 10 days after the procedure. Treg flow assay was performed to determine Treg recruitment by analyzing CD4+CD25+FoxP3+ cells. (a, c, e, g) Flow analysis results from control tissues and (b, d, e,f) Flow analysis results from implant tissue.

Flow cytometry results are given in **Figure 3.4** for PBS-treated control animals and **Figure 3.5** for multicellular organoid-implanted animals. % FoxP3+ cells in the CD4+ cell population indicates presence of Tregs in the analyzed tissue. Compared to only PBS-injected control animals, we found more than 5-fold increase in Treg population at the implantation site (**Figure 3.6**). Additionally, when we compared Treg populations between right (control) and left (implantation site) abdominal tissues in  $\beta$ -TC-6:HSC-CCL22 organoids-implanted animals, we have seen that Tregs were selectively recruited to graft site, where almost 7-fold increase in Treg population was observed. Significant increase in Treg recruitment towards  $\beta$ -TC-6:HSC-CCL22 organoids-implanted site was observed in STZ-induced diabetic animal model.

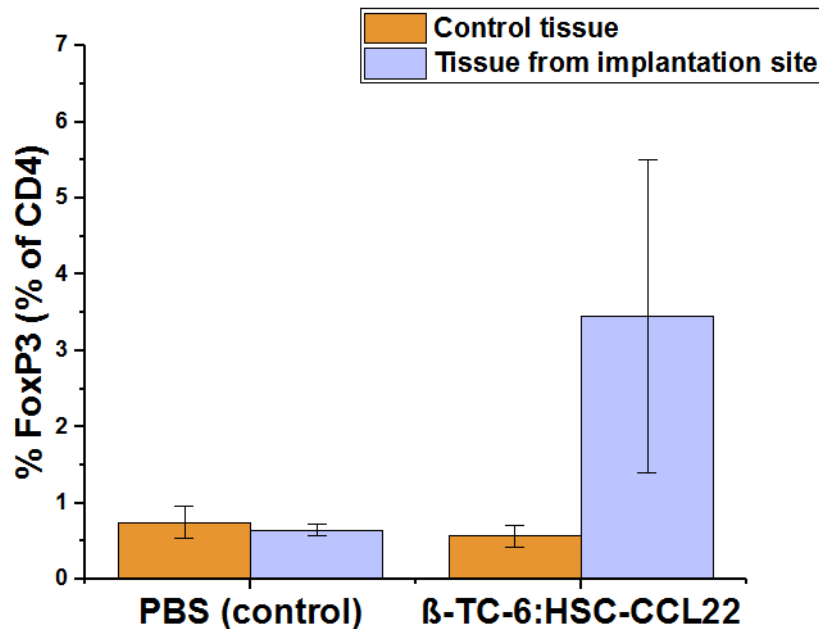


**Figure 3. 6.** Treg recruitment in vivo. % FoxP3+ cells in CD4+ cell population indicates presence of Tregs in the tissues.

### 3.4. Conclusion and Future Work

In this *in vivo* study, we engineered insulin-secreting islets composed of  $\beta$  cells and hepatic stellate cells, which have the ability to secrete CCL22 protein for Treg recruitment. Treg recruitment plays a key role in cancer development, where cancer cells avoid attacks from other immune cells by recruiting Tregs and forming a local biological barrier around themselves. Based upon this capability of cancer cells, we have transfected HSCs with CCL22 gene. Multicellular organoids

prepared with  $\beta$ -TC-6 and CCL22 transfected HSCs were implanted to diabetic mice and implanted tissues were analyzed for Treg recruitment. We found increased number of Treg population in the presence of HSC-CCL22 cells which strongly suggested that Treg recruitment towards implantation site was achieved selectively. For the evaluation of Treg recruitment, 50,000 cells were analyzed by flow cytometer for each experimental group. For multicellular islet organoids-implanted groups, approximately 35% (15,000 cells) of these cells were marked CD4 positive, including T cells and Tregs. Among these 15,000 cells, 5.5% of them (750-900 cells) were marked CD4<sup>+</sup> CD25<sup>+</sup> FoxP3<sup>+</sup>, indicating Tregs. Typical range of Tregs in CD4<sup>+</sup> population is 4-9% [62]. We have managed to recruit 5.5% Tregs to implant site, which is in the typical range of Treg population in all CD4<sup>+</sup> cells. As a future work to investigate whether the number of recruited Tregs is sufficient for graft survival, tissues can be retrieved from animals at extended time points, such as on the 20<sup>th</sup> and 30<sup>th</sup> days to elucidate and comment on Treg amount. To maximize Treg recruitment, CCL22 expressing HSCs can also be co-transplanted alongside with multicellular islet organoids. Additionally, *in vivo* experiments with more control groups, including only  $\beta$ -TC-6 organoids and  $\beta$ -TC-6:HSC-GFP organoids, will be done. Additionally, reversal of diabetes will be investigated by measuring blood glucose levels of diabetic mice after implantation.

## Chapter 4

# Coating of Insulin Secreting $\beta$ -cell Organoids with Lipid Containing Microgels

### 4.1. Introduction

Type 1 diabetes (T1D) is a chronic, immune-mediated pancreatic disease, precipitated by destruction of  $\beta$  cells in pancreas. T1D has severe medical consequences, such as amputation, blindness and renal failure [21]. Most of the patients diagnosed with T1D gets insulin treatment, in which blood glucose (BG) levels are adjusted by exogeneous insulin injections. However, repetitive insulin therapy is not only exhausting for the patient but also not an end-point solution to the disease since it only helps avoiding diabetic complications. Alternatives for the treatment are pancreas and islet transplantation.

Following the Edmonton Protocol [132], where islet allografts were infused to recipients through portal vein and normal BG levels were attained for a long period, many clinical studies were done using isolated cadaveric human islets. Formerly regarded as an experimental and a rare strategy, islet transplantation is now a worldwide accepted routine treatment option with high efficacy. Today, more than 1,500 patients have received islet transplants and approximately 60% of these patients became insulin independent in 5 years. [133]. However, islet performance is jeopardized during isolation and purification procedures since crucial extracellular matrix (ECM) proteins and vasculature are damaged after collagenase digestion [11]. Following the biological stress caused by the isolation process and the attacks from immune system components, implanted islets struggle to remain viable and functional. Once islets are exposed to blood components, chemokines and inflammatory factors are released which leads to instant blood mediated inflammatory reactions (IBMIR) in the vicinity of islets, ultimately causing graft rejection and loss [134].

Transplanted islets are prone to experience rejection from host-body, unless an immunosuppressive therapy is applied. Although immunosuppressive therapy can contribute to islet survival by inhibiting allorejection and autoimmune recurrence, immunosuppressive drugs weaken the immune system of the patient, thereby making them open targets to severe adverse effects [135, 136].

To illuminate the processes behind function and immunoisolation of islets in T1D treatment, researchers mostly make use of rats and mice [137]. On the other hand, with the discovery of new insulin-secreting cell lines that resemble human  $\beta$  cell characteristics, more feasible research can be done. When these cell lines are in adherent monolayer state, their response to glucose is weak. It is conclusively accepted that  $\beta$ - $\beta$  cell interactions, including cell adhesion molecules (CAMs), gap junctions and paracrine signaling, play a key role in insulin secretion activity of islets. To mimic native islets, 3D  $\beta$ -cell spheroids with a variety of in vitro culture techniques can be fabricated. It was shown that mouse islets and organoids prepared with MIN6 cells had similar size, morphology and stimulation indices [138]. Therefore, construction of  $\beta$ -cell spheroids using single  $\beta$  cells is an eligible strategy for islet therapy research in T1D.

Immunoisolation of islets is a golden standard to eliminate exhaustive immunosuppression treatment after islet transplantation. To that end, various encapsulation and coating techniques have been considered for islets. The concept of islet coating is to form a protective barrier around islet transplants which shields them from immune responses. This permselective membrane should supply a hydrated microenvironment in which islets can secrete factors and signals for their metabolic activities such as proliferation and migration [139]. In addition, immunoisolation materials should be biocompatible, non-cytotoxic, and in some cases, biodegradable. Due to their many advantageous properties, such as swelling, inertness and hydrophilicity, poly (ethylene glycol) PEG hydrogels have gained attention as immunoprotected barriers for islets [140]. PEG hydrogels are extensively studied for islet coating and encapsulation. A photopolymerizable derivative of PEG, poly (ethylene glycol) diacrylate (PEGDA), is a versatile material due to its highly modifiable and inert nature. For example, to mimic the microenvironment of islets, PEG hydrogel was functionalized with a variety of peptides, including glucagon like peptide-1 (GLP-1), IKVAV and RGDS. It was shown that combination of peptides improved insulin secretory response of encapsulated islets within this microenvironment [95].

The thickness of immunoisolation membrane is a critical factor for clinical applications of islet transplantation. Macro- and microencapsulation of islets highly

increases the total implant volume. For instance, when islet diameter is increased by 5-fold after microencapsulation, the volume is increased by 125-fold [141]. This volume increase limits the number of islets that can be transplanted in one procedure and might necessitate recurrent transplantations. Therefore, ultra-thin coating alternatives, including conformal coatings and layer-by-layers, have been emerged which minimizes the coating thickness and maximizes the efficiency in the clinical setting.

Islet surface can be engineered by various approaches, such as covalent conjugation, electrostatic or hydrophobic interactions. Covalent conjugation of materials to islet surface could be cytotoxic and cause loss of function because the chemical modifications of cell membrane may disturb cell membrane proteins [142]. On the other hand, non-covalent immobilization methods including hydrophobic interactions have no unfavorable effects on islet function and viability. For example, PEG-lipid derivatives are widely explored polymers for islet and cell surface engineering applications through hydrophobic interactions between phospholipid bilayer of cell membrane and lipid moieties in the PEG chain [102, 141, 143-146]. In addition, by modifying PEG-lipids with other functional groups such as biotin, streptavidin, dibenzocyclooctyne (DBCO) and azide, multilayered membranes and living-cell immobilization on islet surface can be achieved [109, 111].

In addition to ultra-thin conformal coatings, nano and microparticles can be considered as immunoisolation materials. Due to their spherical shapes, nano and microgels have high surface-area-to-volume-ratios, thus presentation of functional ligands is enhanced. Deposition of particles onto islet surface is a recently emerged strategy and not many studies were reported on this subject. For example, mouse islets were firstly PEGylated using EZ-Link Amine PEG<sub>11</sub>-Biotin and then avidin coated poly lactic-co-glycolic acid (PLGA) nanoparticles were deposited on the surface. *In vitro* studies showed that PEGylation and nanoparticle coating of mouse islets improved their structural integrity for long periods. *In vivo* studies conducted with STZ-induced diabetic C57BL/6 mice indicated that this strategy can extend islet functionality, where 4 of 7 mice had normalized BG levels for more than 100 days after nanoparticle coating [147]. Sequential covalent coating of MIN6 spheroids with cholesterol bearing pullulan (CHPOA) nanogels was done and very similar function

and viability was achieved compared to non-coated control groups [76]. Although not a coating study, Headen et al. co-transplanted islets with microgels containing apoptotic form of the Fas ligand (FasL) and reported prolonged survival of the islet grafts in STZ-induced diabetic mice [72]. In their approach, researchers made use of FasL-mediated apoptosis of T cells and provided an immune privileged microenvironment for islets.

In this study, we have investigated coating of  $\beta$ -TC-6 islet organoids with PEG-lipid microgels through hydrophobic interactions. PEG microgels were synthesized via water-in-water (W/W) emulsion technique and their size was optimized by tuning the emulsification and photopolymerization parameters. After microgel optimizations, lipid groups were introduced to hydrogel formulation for hydrophobic deposition of microgels to islet organoid surface. This chapter describes an exclusive coating strategy where all reaction steps take place in aqueous mediums at physiological pH. Additionally, by utilizing hydrophobic interactions between the phospholipid bilayer on cell surface and lipid groups on PEG microgels, coating was achieved without any irreversible modifications that may induce perturbing effects on cell membrane. Coated  $\beta$ -TC-6 islet organoids retained their insulin secretory response and viability. This approach holds promise for immunoisolation by generating an ultra-thin protective barrier around islet organoids where islet transplantation volume is kept minimum.

## **4.2. Experimental**

### **4.2.1. Preparation of PEG Hydrogel Prepolymer Solutions**

PEGDA (Laysan Bio, 10 kDa) was dissolved in 2 mL dH<sub>2</sub>O to a final concentration of 6% (w/v). 37 mM 1-vinyl-2-pyrrolidinone (NVP, Sigma-Aldrich), 225 mM triethanolamine (TEA, Merck), and 0.05 mM Eosin-Y (Sigma) was added to prepolymer mixture. Acr-PEG-DSPE (Biochempeg, 3.4 kDa) was added to prepolymer mixture to a final concentration of 2.5 mM or 5 mM for lipid functionalization. pH of prepolymer solution was adjusted to 8 using 6N HCl. For fluorescence-labeled microgels, fluorescence-o-acrylate (100  $\mu$ g/mL) (Sigma) was included in prepolymer solution. Prepolymer solutions were stored at 4°C until use.

### **4.2.2. Microgel Synthesis**

Microgels with lipid functionality were synthesized by W/W emulsion technique (**Figure 4.1**). Dextran (40 kDa, Sigma) was dissolved at a concentration of

40% (w/v) in a buffer containing 0.22M KCl and 10 mM sodium phosphate and pH was adjusted to 8 with 6N HCl. 2.5 mL of dextran solution was pipetted into a glass vial and 0.5 mL of PEGDA prepolymer solution was added into this solution drop by drop.

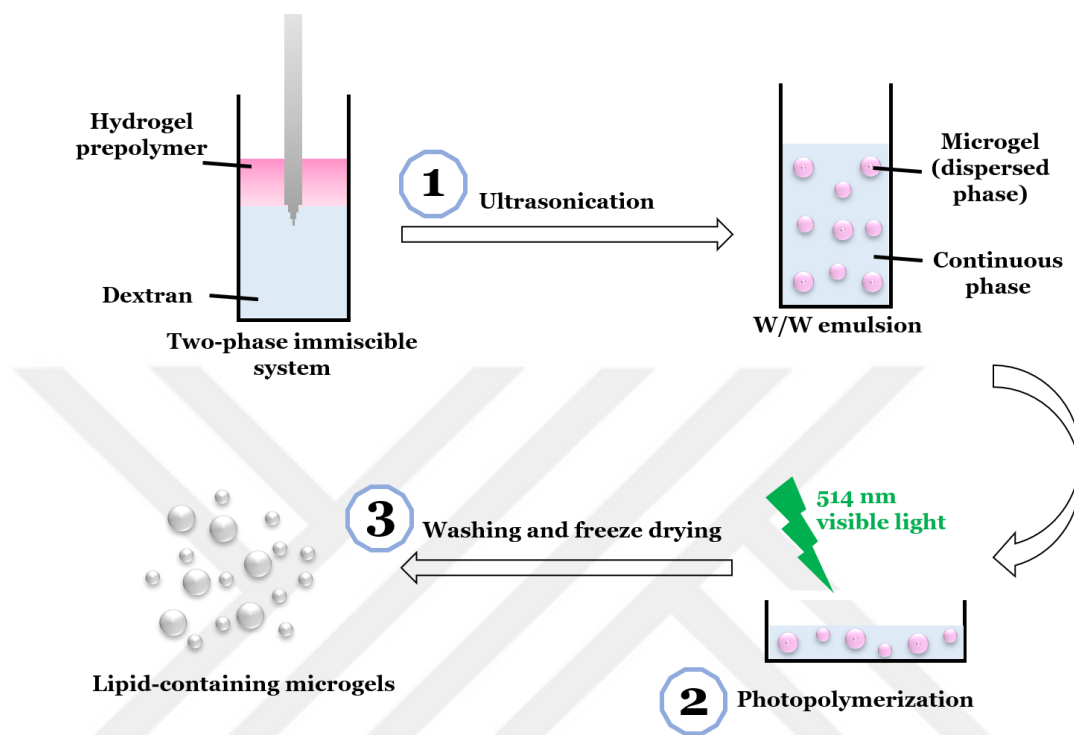


**Figure 4. 1.** Microgel synthesis by W/W emulsion

Solutions were emulsified by an ultrasonic homogenizer (Bandelin Sonopuls) in an ice bath where temperature was kept between 10-15 °C. Different ultrasonic powers (30% and 60%) and emulsification durations (10, 30, 45 minutes) were used for microgel size optimizations. Emulsified PEGDA/dextran solution was kept in dark for 5 minutes for stabilization. Following emulsion stabilization, 750  $\mu$ L of emulsion was photopolymerized with 514 nm visible light at a flux of 5 mW/cm<sup>2</sup> using an argon ion laser (Coherent Inc., Santa Clara, CA) for different laser exposure times (1, 1.5, 2.5, 3 minutes) under stirring. After laser exposure, microgels were transferred to 15 mL conical tubes, 15x diluted with dH<sub>2</sub>O and washed with dH<sub>2</sub>O using 50 kDa Amicon Ultra centrifugal filters (Millipore, Merck) by centrifuging at 3500 rpm for 20 minutes. Washing steps were repeated for 3 times. Next, microgels were frozen and lyophilized for storage at -20°C until use. Microgel size distributions were determined by Image J using brightfield microscopy images captured after laser exposure. For each

experimental condition, approximately 1000 microgels were visually analyzed for size determination.

#### **4.2.3. Visualization of Microgels**

Microgels were imaged by FE-SEM (Zeiss Ultra Plus, Bruker). Lyophilized microgels were coated with 10 nm gold and imaged at 5 kV acceleration voltage. Images of fluorescently labeled microgels were captured under fluorescent microscopy (Nikon). For fluorescent imaging, wet microgels before and after washing steps were used.

#### **4.2.4. Cell Culture**

$\beta$ -TC-6 cells were purchased from ATCC. Cells were cultured in DMEM (HG, Gibco) medium supplemented with 10% FBS, 5% penicillin-streptomycin (Sigma), 5% L-glutamine (Sigma) and 5% sodium pyruvate (Lonza) at 37°C and 5% CO<sub>2</sub> incubator. Medium was refreshed every 3 days and cells were subcultured once a week.

#### **4.2.5. $\beta$ -TC-6 Islet Organoid Formation**

$\beta$ -TC-6 islet organoid organoids were prepared by hanging drop method (**Figure 4.2A**).  $\beta$ -TC-6 cells (P26-33) were grown in 6 cm tissue culture dishes (Nest). At 80-90% confluency, cells were detached from the dishes by trypsinization. Cells were counted under hemocytometer and cell density was adjusted to 300 cell/30 $\mu$ l medium. 30  $\mu$ L droplets of cell suspensions were pipetted onto the lids of 10 cm culture dishes (TPP) by a microchannel micropipette (Eppendorf). Next, the lids were gently inverted back to plates containing 8 mL sterile PBS and 80  $\mu$ L penicillin streptomycin (PS). Hanging drops were incubated for 3 days at 37°C and 5% CO<sub>2</sub>.

#### **4.2.6. Coating of $\beta$ -TC-6 Organoids With PEG-Lipid Microgels**

Lyophilized microgels with different lipid concentrations (2.5 mM and 5 mM) were resuspended in sterile 1X PBS at various concentrations (10 mg/mL and 20 mg/mL), mixed by vortex and filter sterilized using 0.22  $\mu$ m syringe filters (Aisimo). Following 3-day incubation, hanging drops were disrupted by pouring PBS/PS mixture onto the droplets. 200 islet organoids were hand-picked and transferred to a 5-mL sterile polypropylene tube (Greiner Bio One). Excess PBS was removed by careful pipetting and 800  $\mu$ L of microgel solution was added to 200 islet organoids. Islets were incubated for 1h to allow the interactions between phospholipid bilayer of cell

membrane and DSPE groups in microgels. During incubation, polypropylene tubes were gently shaken every 15 minutes.

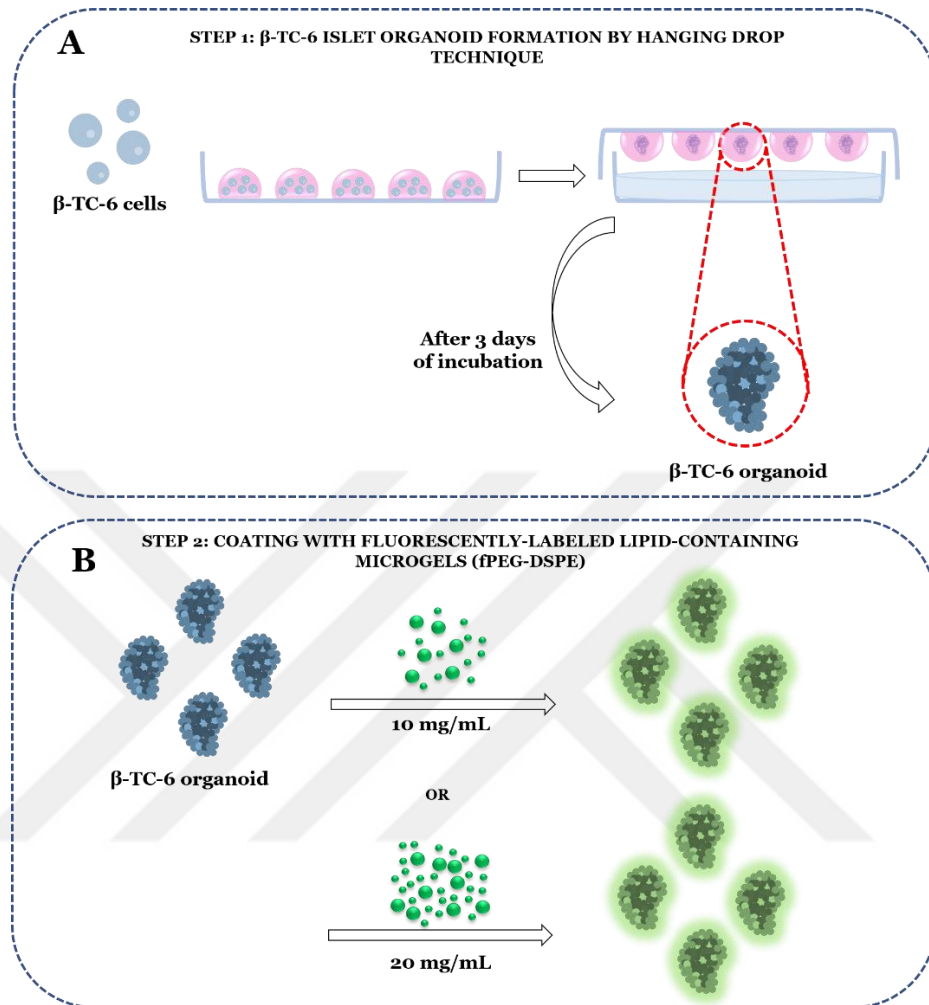


**Figure 4. 2.**  $\beta$ -TC-6 organoid formation and coating of organoids. A) Organoid formation by hanging drop technique. B) Coating of organoids with fluorescently-labeled microgels at various concentrations (10 and 20 mg/mL).

Following the incubation, islets were washed 3 times with PBS and growth medium. For the confirmation of coating, fluorescently labeled microgels were used (**Figure 4.2B**). Coated organoids were imaged under fluorescent microscope. Images were acquired at the same exposure and analog gain values for comparison. Images were processed with Image J for islet surface area and diameter calculations.

#### 4.2.7. Viability of Microgel Coated $\beta$ -TC-6 Organoids

Islet organoid viability was evaluated by live/dead (green/red) staining using fluorescein diacetate (FDA) and propidium iodide (PI). For FDA/PI staining, unlabeled PEG microgels were used. Briefly, following the coating step, 30-40 islet organoids were hand-picked under microscopy.  $\beta$ -TC-6 organoids were stained with

8.5  $\mu\text{g}/\text{mL}$  PI and 42.4  $\text{ng}/\text{mL}$  FDA. After 5 minutes of incubation at dark,  $\beta$ -TC-6 organoids were washed twice with 1X PBS. Next, they were imaged under fluorescence microscope. FDA/PI staining was done on the day of coating and on the next day. For day 2 analysis, coated islets were incubated for 24 hours under standard culture conditions in growth medium and the next day, the same staining procedure was applied.

#### **4.2.8. Metabolic Activity of Microgel Coated $\beta$ -TC-6 Organoids**

Metabolic activity of coated and non-coated  $\beta$ -TC-6 organoids was assessed with Cell Titer Glo (Promega) for intracellular ATP levels and Caspase 3/7 Glo (Promega) for caspase activity. Both assays are luminescent assays and for Cell Titer Glo assay, luminescence intensity is directly proportional to ATP, which is also proportional to the number of living cells. For Caspase 3/7, luminescence is directly proportional to caspase activity.

For Cell Titer Glo luminescence assay, a standard curve of ATP was formed using different ATP concentrations and 120  $\mu\text{l}$  of these solutions were transferred to 96-well plates in duplicates. Next, 10  $\beta$ -TC-6 organoids (coated and non-coated) were hand-picked in 120  $\mu\text{l}$  growth medium and transferred to 96-well plate. 60  $\mu\text{L}$  of Cell Title Glo reagent was added on ATP standards and organoids. Organoids were incubated at dark, shaking at 200 rpm for 15 minutes. Following the incubation step, ATP levels were read on a microplate reader (Synergy H1 Hybrid Multi-Mode Microplate Reader, Bio-Tek).

For Caspase 3/7 Glo luminescence assay, 10  $\beta$ -TC-6 organoids (coated and non-coated) were hand-picked in 120  $\mu\text{l}$  growth medium and transferred to 96-well plate. 60  $\mu\text{L}$  of Caspase 3/7 Glo reagent was added on organoids. 96-well plate was shaken for 30 seconds at 400 rpm and then incubated statically for 1.5 hours at RT and at dark. Following the incubation step, caspase activity was read on a microplate reader (Synergy H1 Hybrid Multi-Mode Microplate Reader, Bio-Tek).

#### **4.2.9. Functionality of Microgel Coated $\beta$ -TC-6 Organoids**

Insulin secretory responses of coated and non-coated organoids were evaluated by static incubation in low glucose (LG, 2.8 mM) and high glucose (HG, 28 mM) Krebs-Ringer buffers (KRB). Briefly, LG and HG buffers were transferred to a 24 well plate and 12  $\mu\text{m}$  cell culture inserts (Millipore) were placed in each well. Firstly, 20  $\beta$ -TC-6 organoids (coated and non-coated) were placed in culture inserts in LG KRB and

incubated for 1h. The first LG incubation is done to adjust organoids to a low glucose microenvironment since they are cultured in a HG growth medium. Next, inserts were transferred to a second set of LG buffers. After 1h of incubation, inserts were finally transferred to HG buffer. Following 1h incubation in HG buffer, LG and HG buffers were stored at  $-20^{\circ}\text{C}$  until analysis with mouse insulin ELISA kit (Mercodia). ELISA analysis was done by following the manufacturer's instructions. Functionality of microgel coated and non-coated  $\beta$ -TC-6 organoids was assessed by calculating stimulation index (SI) which is the ratio of the insulin amount in LG buffer to insulin amount in HG buffer after static incubation.

### **4.3. Results and Discussion**

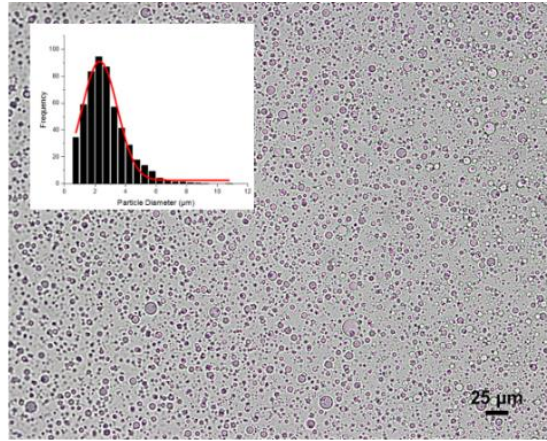
#### **4.3.1. PEG Microgel Synthesis by Water-in-Water (W/W) Emulsion and Photopolymerization**

PEG microgels were synthesized by W/W emulsion technique. As continuous phase, 40% (w/v) dextran solution was selected. PEG and dextran solutions form two distinct phases when polymer concentrations are above a critical value [148]. This two-phase system was then emulsified by ultrasonic homogenizer. Sonication process creates acoustic cavitation in PEG/dextran mixture and PEG droplets are dispersed in dextran phase. Next, emulsions were photopolymerized under 514 nm visible light and PEG microgels were formed.

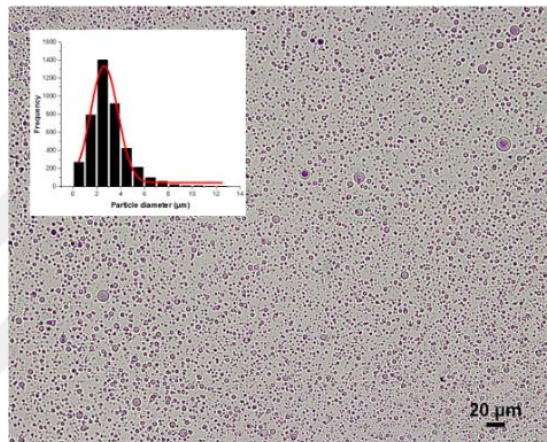
##### **4.3.1.1 Effect of Ultrasonication Parameters on Microgel Diameter**

Here, we investigated the effect of ultrasonication parameters on microgel size by altering sonication power densities (30% and 60%) and time (10, 30, 45 minutes). **Figure 4.3** and **Figure 4.4** show microscope images of PEG microgels generated by 30% and 60% ultrasonication power, respectively.

10 min



30 min



45 min

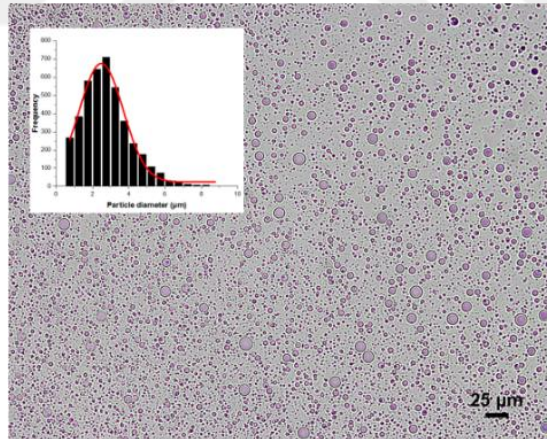


**Figure 4. 3.** Microscope images of PEG microgels prepared by emulsification at 30% homogenizer power. Images were captured after laser exposure. Insets represent size distribution histograms of microgels. Size distributions were calculated by Image J using microscope images at 20x magnification.

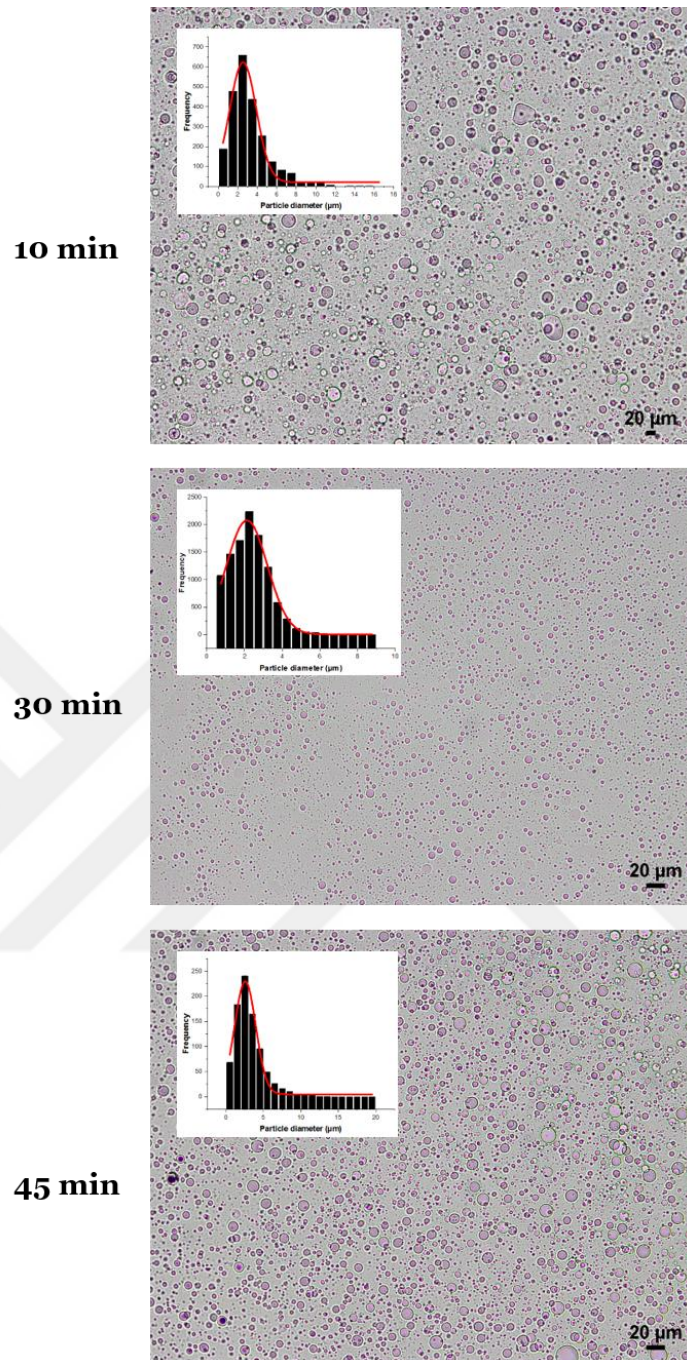


**Figure 4. 4.** Microscope images of PEG microgels prepared by emulsification at 60% homogenizer power. Images were captured after laser exposure. Insets represent size distribution histograms of microgels. Size distributions were calculated by Image J using microscope images at 20x magnification.

In both cases, increasing ultrasonication time from 10 to 30 minutes decreased microgel diameter (from  $2,31 \pm 0,041 \mu\text{m}$  to  $2,29 \pm 0,059 \mu\text{m}$  for 30% power and from  $2,54 \pm 0,07 \mu\text{m}$  to  $2,13 \pm 0,039 \mu\text{m}$  for 60% power) (**Figure 3.5**). When ultrasonication time was extended to 45 minutes, microgel diameters were significantly increased for

both cases (to  $2,48 \pm 0,038 \mu\text{m}$  for 30% power and to  $2,547 \pm 0,060 \mu\text{m}$  for 60% power) (Figure 3.5).

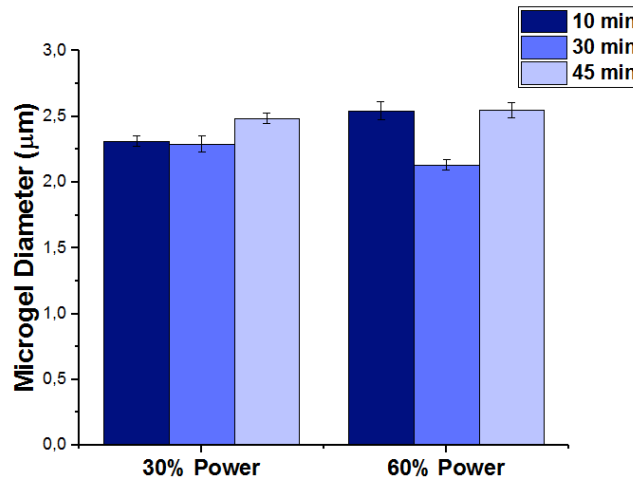


**Figure 4. 5.** Microgel diameters after tuning ultrasonication parameters.

Emulsion is assembled when a mechanical mixing force is applied to aqueous two-phase systems. In our case, ultrasounds create micron size PEG droplets that are thoroughly dispersed in dextran phase. This W/W emulsion system is highly dynamic; in which separation and coalescence of micro-droplets occur continuously. Therefore, diameter of these droplets is vastly determined by the rate of separation and coalescence during emulsification. Physical properties of both phases as well as ultrasonication conditions affect this phenomenon [149]. Higher microgel diameters can possibly be explained by the dynamism of the emulsion. Increasing sonication time from 30 to 45 minutes may have caused a greater extent of turbulence in emulsion system, where coalescence of micro-droplets occurs more than the separation. In addition, increasing the sonication power from 30% to 60% has possibly created a similar impact on diameter. Our aim here is to use PEG microgels for coating islet organoids. The thickness of immunisolating membrane is an important factor and thinner membranes are desired for their advantageous features such as higher nutrient diffusion rates and smaller implant volumes. Therefore, even though diameters of microgels did not differ from one another considerably, we chose the emulsification conditions which provided us with the smallest microgel diameter ( $2,13 \mu\text{m}$ ), which is 60% power and 30 minutes ultrasonication.

#### 4.3.1.2 Effect of Laser Exposure Time on Microgel Formation

After emulsification, emulsions were photopolymerized via visible light. Prior to photopolymerization, emulsions were kept for 5 minutes for stabilization. Ultrasonication causes turbulence and an equilibrium between segregation and merging of micro-droplets should be reached before photo-crosslinking to obtain more homogeneous size distributions. Therefore, 5-minute stabilization step was included. Following the 5 minutes stabilization, emulsions were exposed to visible light for different durations (1, 1,5 and 2,5 minutes) and immediately after laser exposure, 2  $\mu$ L photopolymerized PEG microgels were pipetted onto a microscope glass and observed under microcopy (**Figures 4.7, 4.8 and 4.9**). Images were captured at 4 different time points,  $t=0$  (right after laser exposure), 30, 60 and 180 seconds.

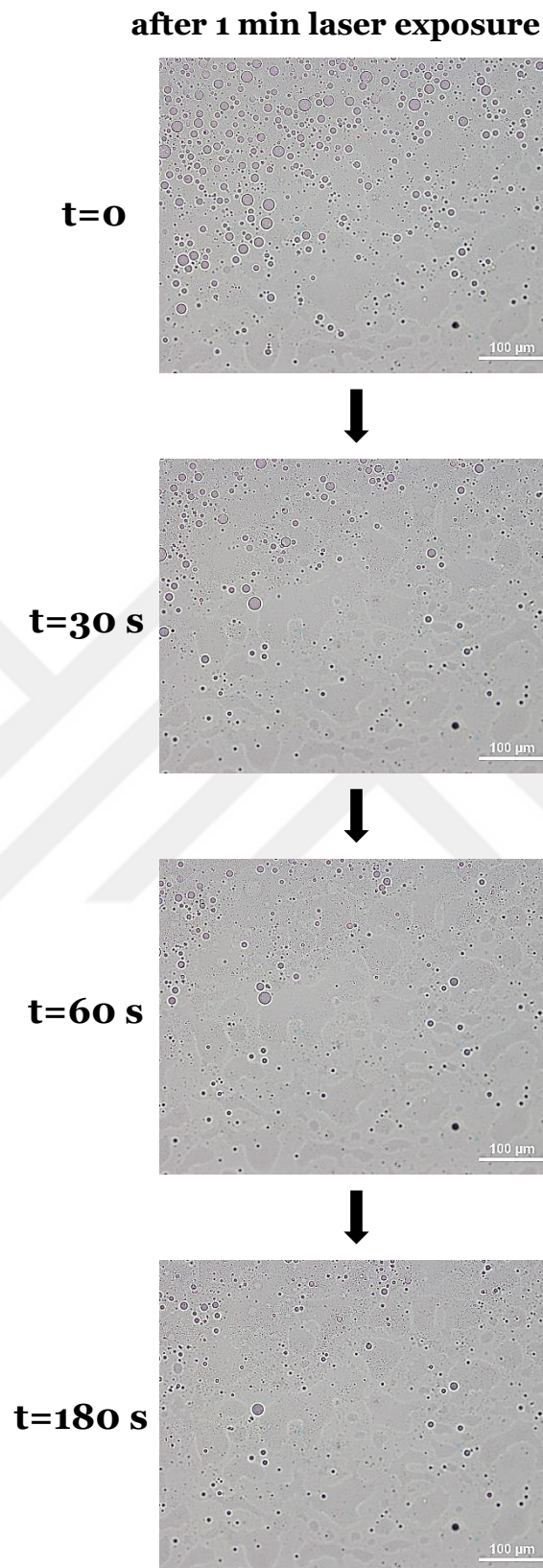
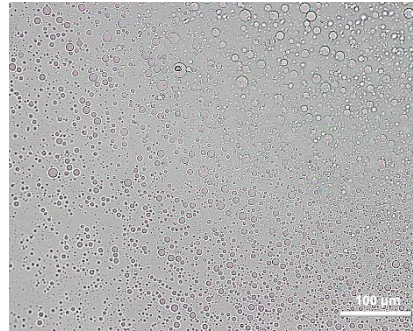


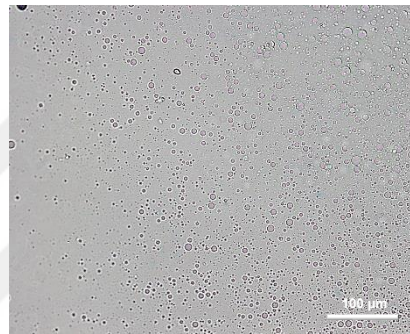
**Figure 4. 6.** Microscope images of photopolymerized PEG microgels. Laser duration = 1 minute. Images were captured right after laser exposure. 4 consecutive images of the same area were captured at different time points (0, 30, 60 and 180 seconds). Scale bars= 100 $\mu$ m.

after 1,5 min laser exposure

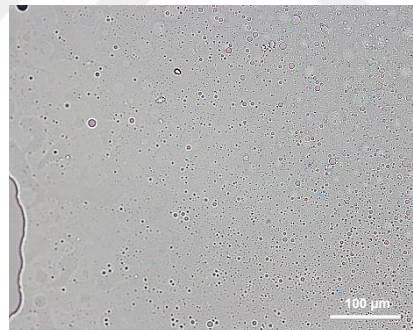
t=0



t=30 s



t=60 s



t=180 s

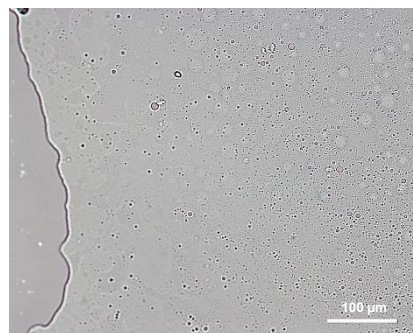
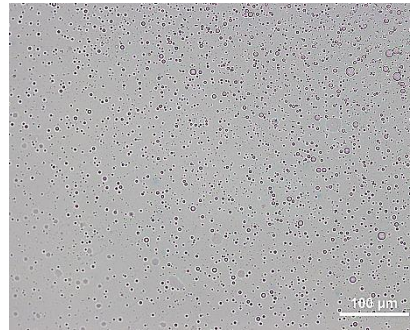


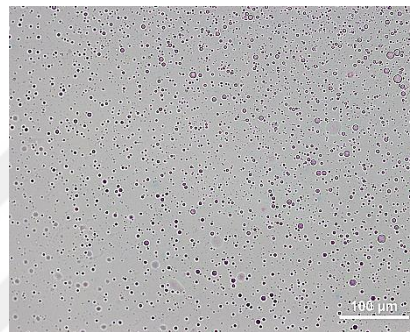
**Figure 4. 7.** Microscope images of photopolymerized PEG microgels. Laser duration = 1,5 minutes. Images were captured right after laser exposure. 4 consecutive images of the same area were captured at different time points (0, 30, 60 and 180 seconds). Scale bars= 100 $\mu$ m.

after 2,5 min laser exposure

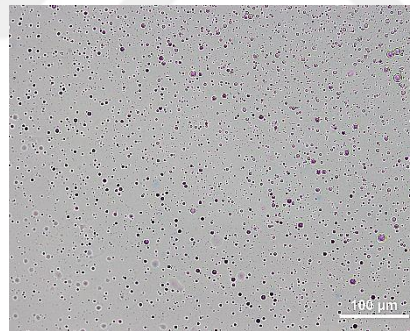
t=0



t=30 s



t=60 s



t=180 s

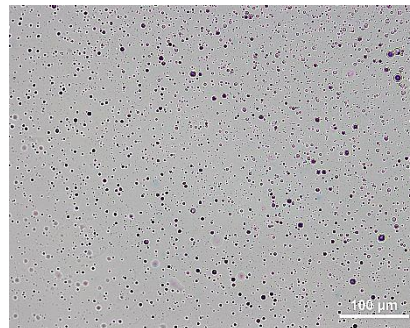


**Figure 4. 8.** Microscope images of photopolymerized PEG microgels. Laser duration = 2,5 minutes. Images were captured right after laser exposure. 4 consecutive images of the same area were captured at different time points (0, 30, 60 and 180 seconds). Scale bars= 100 $\mu$ m.

The goal of this type of image acquisition was to observe how micro-droplets behave after being exposed to a certain amount of energy. We expected to see more stable images in the case of higher laser exposure durations because the duration of laser exposure correlates with the amount of energy transferred to micro-droplets (**Figure 4.6**). In the presence of a suitable photoinitiator, in our case Eosin-Y, PEGDA crosslinks by using light energy to start and propagate the polymerization reaction [150]. When sufficient energy is transferred to emulsions, PEGDA micro-droplets get crosslinked and form stable micron-sized hydrogel particles. In the case of insufficient energy transmission, we expected to see fewer stable images, where micro-droplets were bursting, and ultimately disappearing, since they could not get crosslinked.

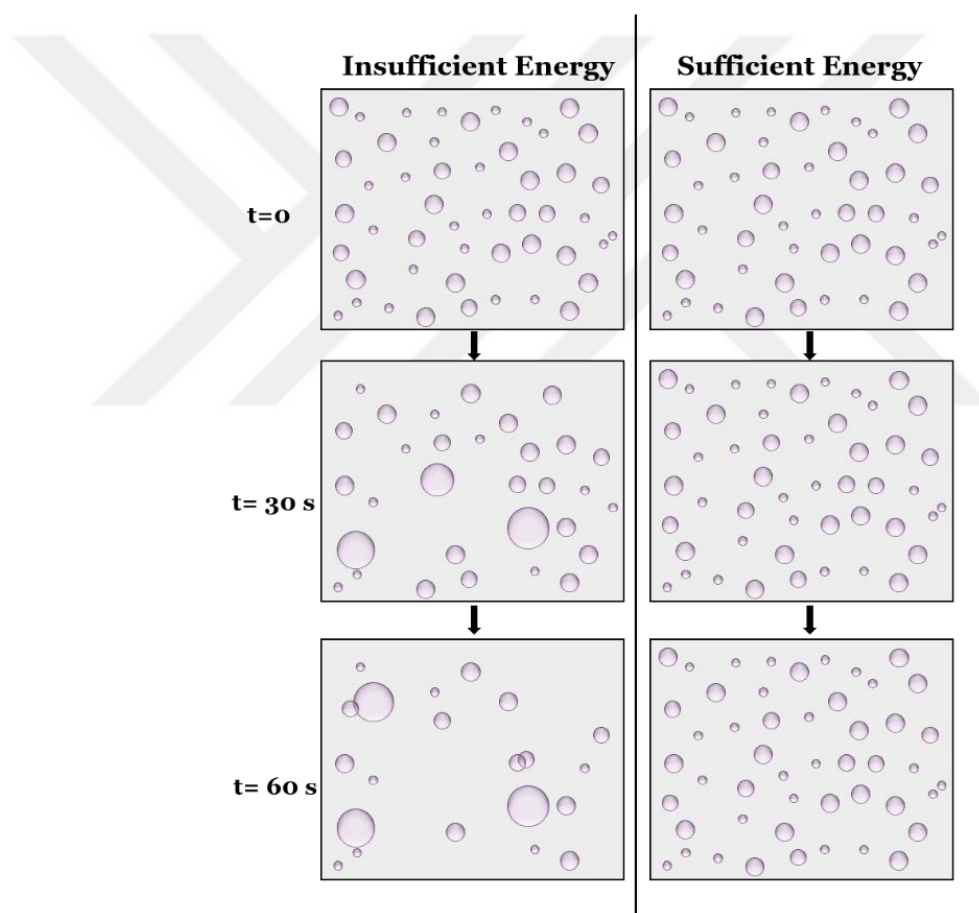


**Figure 4. 9.** Demonstration of the effect of laser exposure on microgel formation. If sufficient energy is transferred to emulsions during photopolymerization, stable microgels are obtained, while insufficient energy causes micro-droplets to burst and disappear since crosslinking efficiency is low.

Indeed, for 1 and 1,5 minutes of laser exposure, microscope images demonstrated that micro-droplets were not crosslinked and started to burst and

disappear (**Figures 4.6 and 4.7**). After 180 seconds, most of the droplets were vanished, indicating they were not crosslinked microgels but rather PEGDA microdroplets. On the other hand, when emulsions were exposed to laser for 2,5 minutes, they were crosslinked and formed stable microgels (**Figure 4.8**).

In addition, we also studied higher laser exposure durations and observed that when laser exposure is longer than 2,5 minutes, microgels tend to aggregate and form bulky structures (**Figure 4.10**). We inferred that excessive laser exposure crosslinks microgel spheres to each other, leading to aggregation. This indicates that the energy transmitted to emulsions for 2,5 minutes was adequate to polymerize PEG microdroplets and turn them into crosslinked microgels.

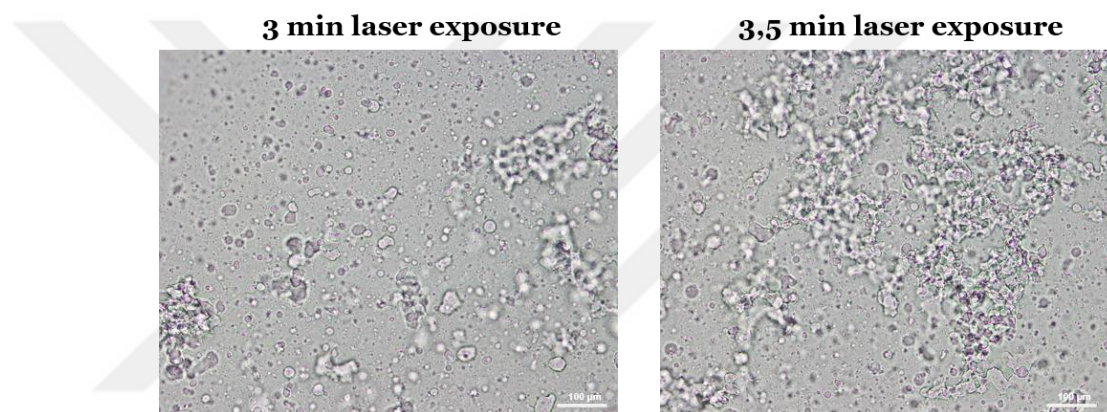


**Figure 4. 10.** Microscope images of photopolymerized PEG microgels. Laser duration = 3 and 3,5 minutes. Images were captured right after laser exposure. Scale bar= 100  $\mu$ m.

#### 4.3.1.3. Morphology and Fluorescent Labeling of PEG Microgels

To characterize size and morphology of PEG microgels, scanning electron microscopy imaging was used. After washing and lyophilization steps, microgels were investigated under FE-SEM (**Figure 4.11**). FE-SEM images demonstrate that microgels have a size distribution of 2-3  $\mu$ m, consistent with measurements from Image J analysis of wet emulsion microscopy images. Sonication parameters do not have significant impact on microgel morphology, since in all conditions very similar spherical hydrogel particles were obtained.

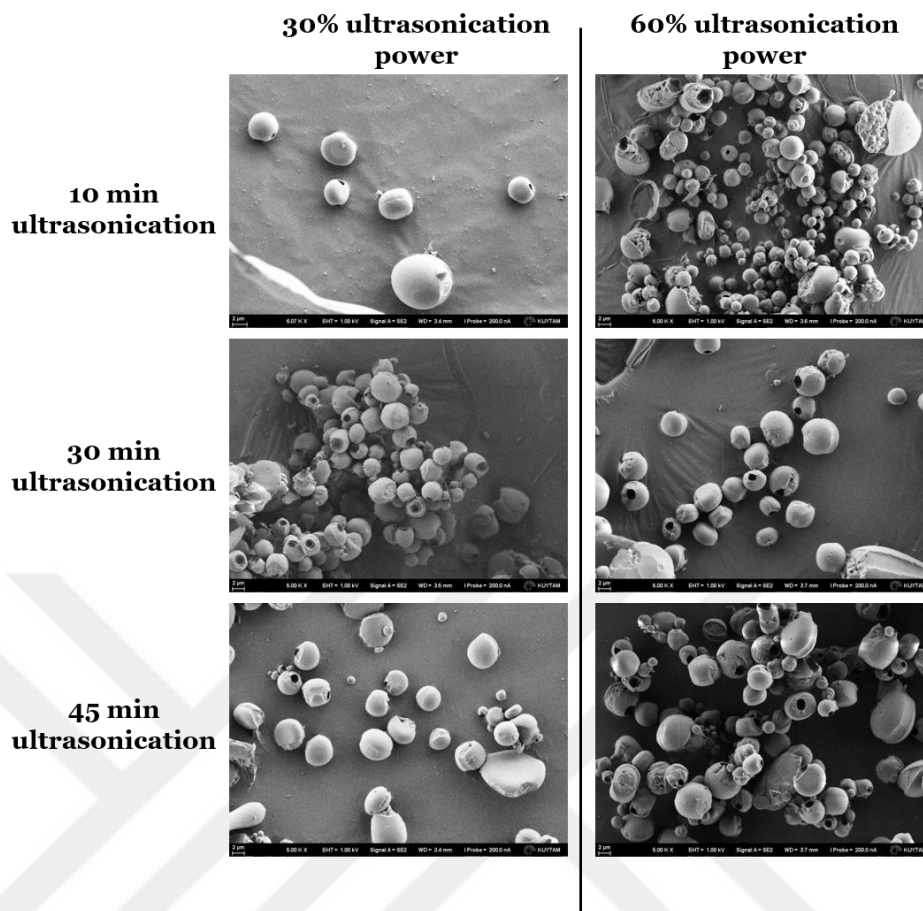


**Figure 4. 11.** FE-SEM images of PEG microgels synthesized with different ultrasonication power densities and durations. Scale bar= 2  $\mu$ m.

For visualization purposes, PEG microgels were fluorescently labeled. Fluorescein-o-acrylate was included in prepolymer solution for labeling microgels. Acrylate groups in PEGDA and fluorescein-o-acrylate react with each other during laser exposure. Fluorescent microscope images of microgels were captured immediately after laser exposure. To confirm the covalent bonding of fluorescent molecule to microgels, images were captured before and after washing steps. In addition, as a control experiment, fluorescein-o-acrylate was added to photopolymerized emulsions after laser exposure and images were captured with fluorescent microscope. Since there is no laser exposure and covalent attachment of fluorescent molecules to PEG microgels, fluorescence intensity is expected to fade in the control group. Fluorescent images of PEG microgels before and after washing indicates that fluorescein-o-acrylate is successfully attached to microgels (**Figure 4.12**).

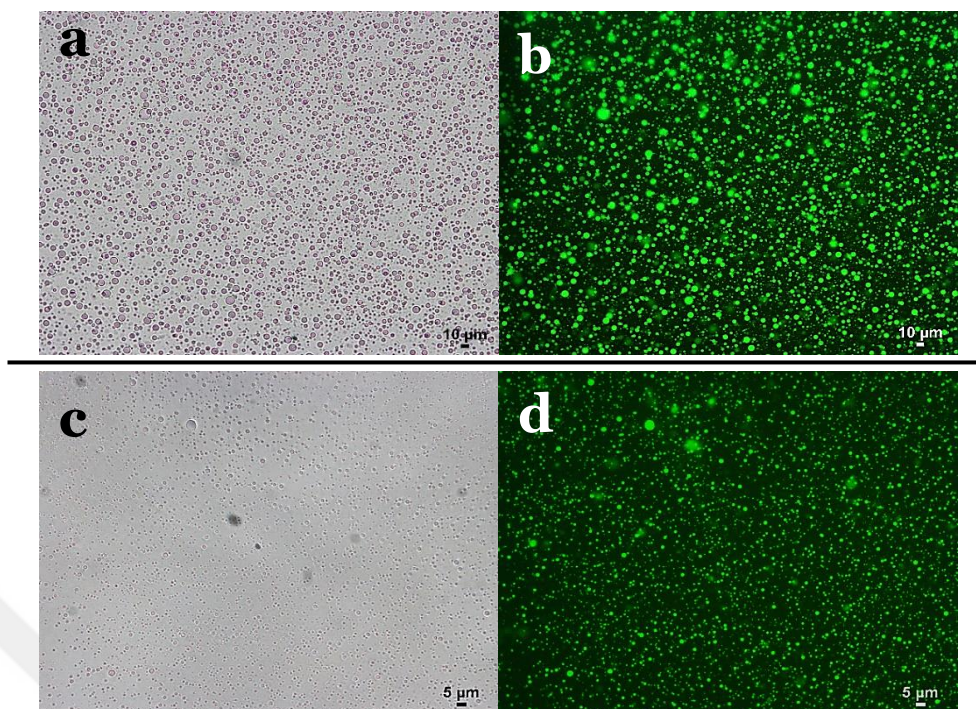


**Figure 4. 12.** Brightfield and fluorescent images of fluorescently labeled PEG microgels synthesized with optimized ultrasonication and laser exposure parameters (60% power, 30 min ultrasonication and 2,5 min laser exposure). Images were captured before and after washing microgels. (a, b) before, (c,d) after washing. Scale bars for a and b = 10  $\mu$ m, c and d =5  $\mu$ m.

The disappearance in fluorescence intensity in control microgels indicates that laser exposure is necessary for covalent attachment of fluorescence-o-acrylate to PEGDA (**Figure 4.13**). The stability of fluorescence signal in labeled microgels suggests that fluorescence-o-acrylate is successfully conjugated to microgel network.

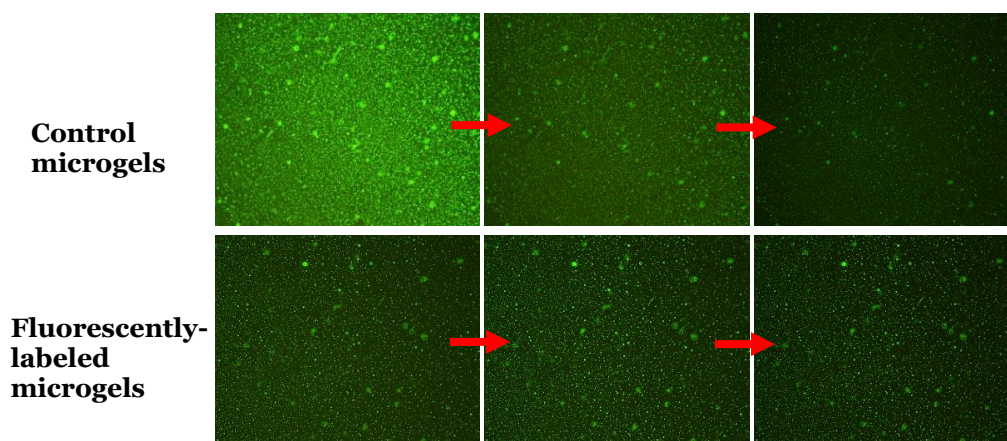


**Figure 4. 13.** Confirmation of fluorescent conjugation to microgels. Fluorescein-o-acrylate was added to microgels after laser exposure as control group. Fluorescence signal fades in control microgels, whereas the signal remains in labeled microgels.

### 4.3.2. $\beta$ -TC-6 Organoid Formation with Hanging Drop and Coating of Organoids with Lipid-containing Microgels

It is established that re-constitution of islets from insulin secreting  $\beta$  cell lines of mice or rat closely mimic the morphology and functionality of native islets [138]. These islet-like structures, also known as pseudoislets, has many advantages for research purposes. Since  $\beta$  cell lines, including MIN6, INS-1,  $\beta$ -TC-6 and RINm5F, are commercially available, researchers can easily make use of them by employing simple 3D cell culture methods to fabricate islet spheroids, which we also call islet organoids. In our study, we used hanging drop technique to form 3D islet organoids with a mouse insulinoma cell line,  $\beta$ -TC-6.  $\beta$ -TC-6 cells are immortalized pancreatic  $\beta$  cells that have epithelial morphology. They secrete insulin in response to glucose and have been used in the literature for reconstitution of islets [151-154]. For organoids formation, 300 cell suspensions were placed on the lids of cell culture plates in 30  $\mu$ L growth medium. The lids were inverted and incubated for 3 days. Following the 3-day incubation, organoids were formed. Each islet organoid contains  $\sim$ 300 viable and functional  $\beta$ -TC-6 cells, held together by intercellular bonds.

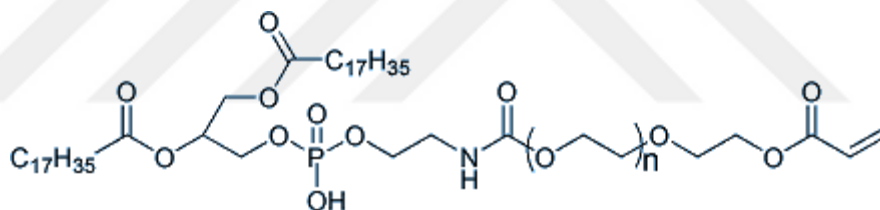


**Figure 4. 14.** Chemical structure of acrylate-PEG-DSPE

We exploited hydrophobic interactions to coat  $\beta$ -TC-6 organoids with lipid-containing microgels. PEG-lipid derivatives were extensively used for the immobilization of immunoprotective membranes to islets without any harm to viability and function [102, 141, 143-146]. We used acrylate-PEG-DSPE, where DSPE stands for 1,2-distearoyl-sn-glycero-3-phosphoethanolamine (**Figure 4.14**). This phospholipid moiety has an alkyl chain that contains 16 methylene units. This long hydrophobic alkyl chain is the mediator of hydrophobic interactions between lipid-containing microgels and islet cell membrane, where alkyl chain is predicted to anchor into phospholipid bilayer of the cell membrane [145] (**Figure 4.15**).

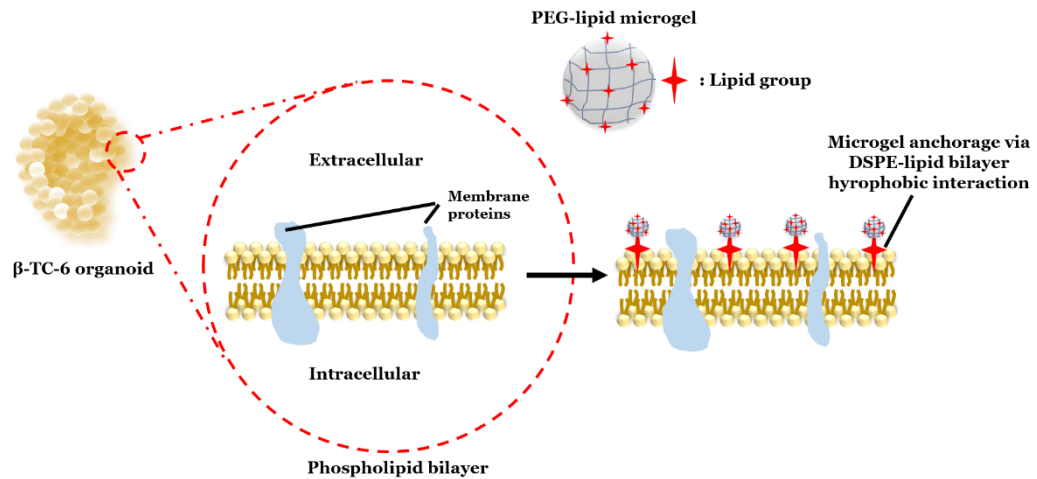


**Figure 4. 15.** Schematic representation of the hydrophobic interaction between PEG-lipid microgels and phospholipid bilayer on cell membrane.

Coating was achieved simply by incubating  $\beta$ -TC-6 organoids with microgel solutions (10 and 20 mg/ml) of different DSPE concentrations (2.5 and 5 mM). To confirm the deposition of microgels around organoids, fluorescently-labeled microgels were used (**Figure 4.16A**). In all experimental groups, green fluorescence was observed, which indicates successful coating of islet organoids. When lipid concentration was doubled, higher fluorescence signals were acquired. Since lipid groups are the anchors of microgels which deposit them onto the surface of organoids, it was expected to see more fluorescence intensity in higher lipid concentration groups. More microgels could cover organoids in 5 mM groups compared to 2.5 mM groups and this was accompanied by increased fluorescence. Increasing the microgel concentration from 10 to 20 mg/mL also raised the coating efficiency. In addition, organoid surface areas and diameters were investigated and calculated (**Figure 4.16B and C**). Diameters are  $134,04 \pm 13,2 \mu\text{m}$ ,  $140,54 \pm 17,8 \mu\text{m}$ ,  $143,8 \pm 17,3 \mu\text{m}$ ,  $142,99 \pm 12,9 \mu\text{m}$  and  $145,26 \pm 15,7 \mu\text{m}$  for control, 2.5 mM DSPE/10mg/mL microgel, 2.5 mM DSPE/20 mg/ml microgel, 5 mM DSPE/10 mg/ml microgel and 5 mM DSPE/20 mg/ml microgel groups, respectively (**Figure 4.16C**). This slight increase in organoid diameter when microgel and lipid concentrations are increased also suggests that coating was accomplished.

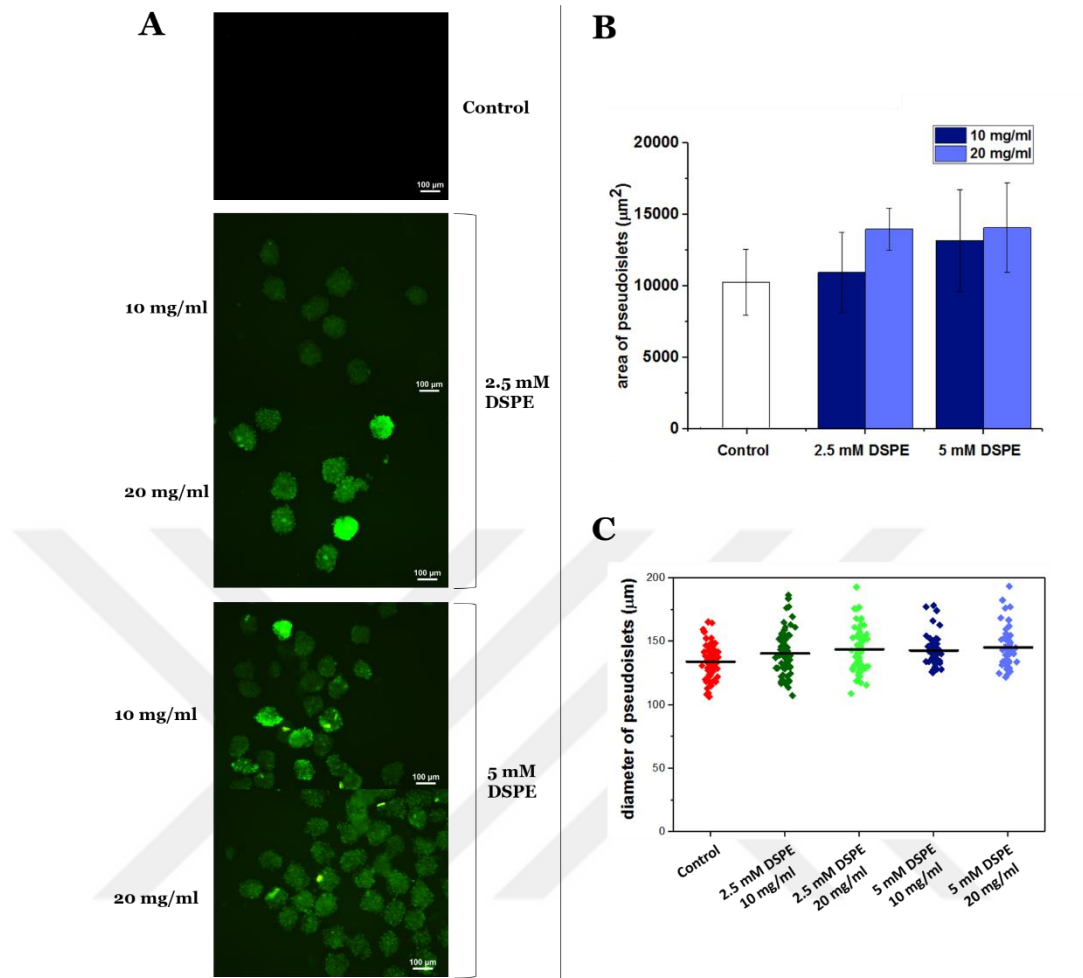


**Figure 4. 16.** PEG-lipid microgel coating of  $\beta$ -TC-6 organoids with different microgel and lipid concentrations. A) Fluorescence images of coated organoids. Scale bars=100 $\mu\text{m}$ . B) surface area and C) diameter of islet organoids.

#### 4.3.4. Viability of Microgel Coated $\beta$ -TC-6 Organoids

Cell viabilities were evaluated by live/dead staining, using FDA (stains viable cells) and PI (stains dead cells) for two consecutive days. In all groups, we observed that the ratio of green area to red area is significantly high, which is a clear indication of cell viability (**Figure 4.17**). In addition, comparing non-coated organoids to coated ones, there is not a significant change in green areas. Coating process takes place in a physiological environment (PBS, pH=7.4) and deposition of microgels occurs via non-covalent hydrophobic interactions. Therefore, we did not expect to encounter any perturbation of cell membrane that may harm cell viability. Indeed, for 2 consecutive days, organoids in all experiment groups gave high green fluorescence intensity compared to red, therefore organoid viabilities were retained for 2 days.

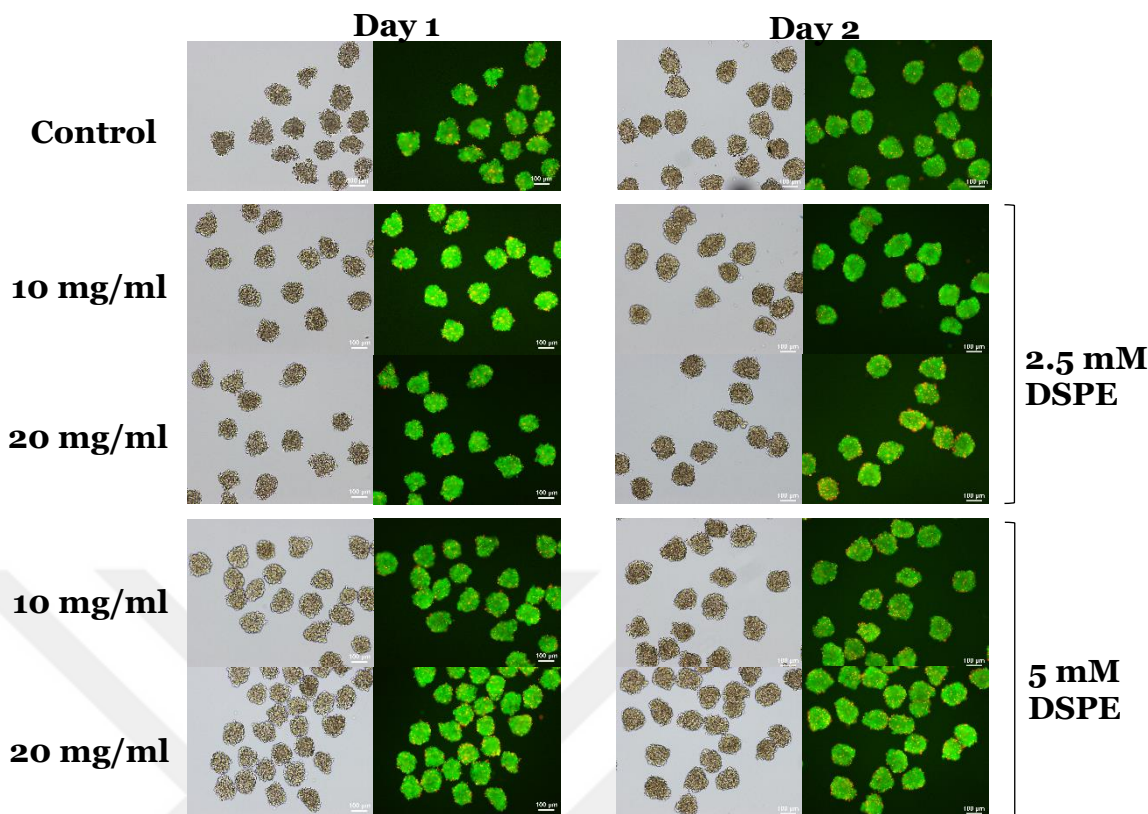


**Figure 4. 17.** Live/dead staining of  $\beta$ -TC-6 organoids after microgel coating. Green: Viable (fluorescein diacetate). Red: Dead (propidium iodide). Scale bars=100 $\mu$ m.

#### 4.3.5. Metabolic Activity of Microgel Coated $\beta$ -TC-6 Organoids

Metabolic activity of non-coated and coated  $\beta$ -TC-6 organoids were investigated by measuring intracellular ATP levels and caspase activities. ATP levels are directly proportional to the number of living cells. Intracellular ATP levels were measured around 0.25  $\mu$ M for all groups (**Figure 4.18A**). Additionally, when ATP levels were normalized to that of non-coated control organoids, percent viabilities were calculated as %88,4 $\pm$ 8, %86,8 $\pm$ 17,2, %99,06 $\pm$ 8,3 and %97,6 $\pm$ 9,2 for 2.5 mM DSPE/10mg/mL microgel, 2.5 mM DSPE/20 mg/ml microgel, 5 mM DSPE/10 mg/ml microgel and 5 mM DSPE/20 mg/ml microgel groups, respectively (**Figure 4.18B**). Interestingly, when DSPE concentration was doubled from 2.5 mM to 5 mM, higher viabilities were observed. This phenomenon can be explained by the role of lipids in cell membrane structures. It was shown that, when INS-1 cells were treated with different concentrations of liposomes, as the lipid concentration increased, metabolic activity of cells also increased [155]. Lipids have a major role in maintaining the integrity of cell membrane and reducing the necrosis of cells. When lipid amount was

doubled from 2.5 to 5 mM, more microgels could deposit on organoids and this may have a positive effect on cellular activity. Organoids treated with 5 mM DSPE containing microgels had higher metabolic activities such as proliferation, which eventually gives higher ATP levels and viabilities.

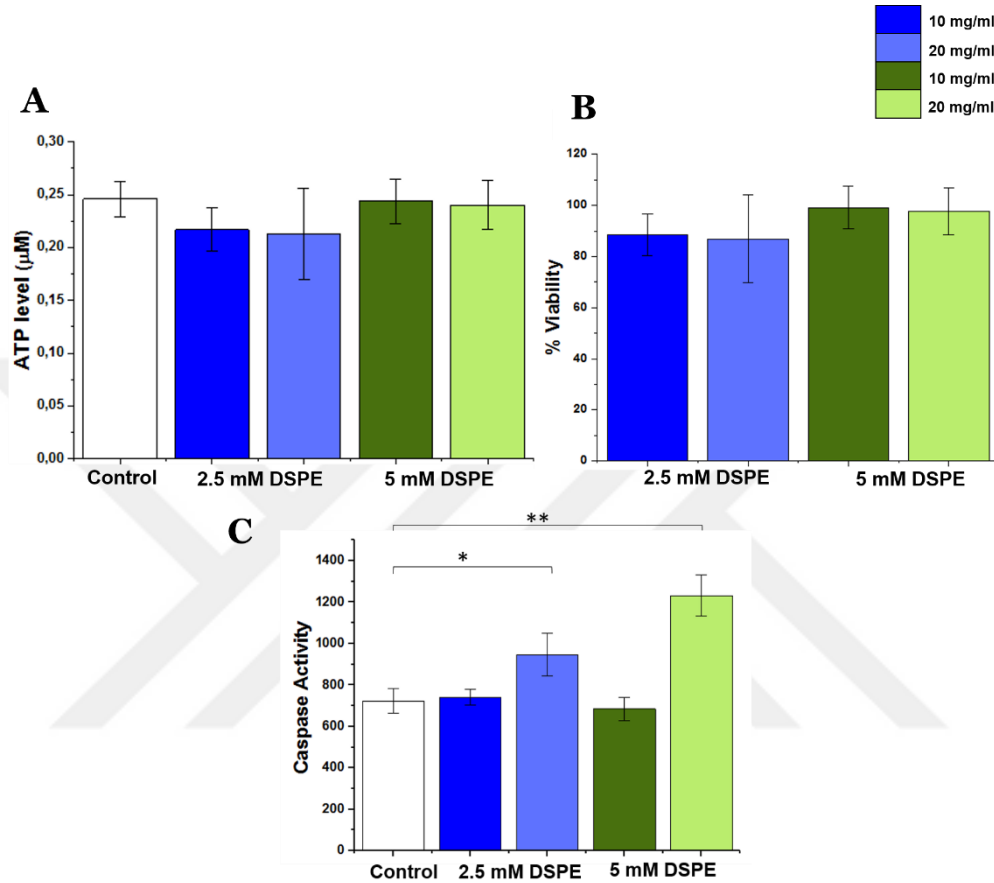


**Figure 4.18.** Metabolic activity of  $\beta$ -TC-6 organoids after microgel treatment. A) ATP levels. B) Percent viabilities and C) Caspase activity of organoids. Percent viabilities and caspase activities were calculated by normalizing values of coated groups to non-coated control group. Mean $\pm$ SD. \*\*p<0.01. \*p<0.05.

Next, we examined the apoptotic activity of non-coated and coated organoids by caspase assay and observed similar results to viability assay, where increases in cell viabilities were followed decreases in caspase activity (**Figure 4.18C**). Unexpectedly, we observed the highest caspase activity for 5 mM DSPE/20 mg/mL microgel treated group. Increasing microgel concentration from 10 to 20 mg/mL might have caused a cytotoxic effect and increased apoptotic activity. Bal et al. have reported that, Increasing pullulan nanogel concentration from 1 to 5 mg/mL also caused higher apoptotic activity for MIN6 pseudoislets [76]. Therefore, increasing the concentration of microgel might have a negative effect on apoptotic activity of  $\beta$  cell organoids.

#### 4.3.6. Insulin Secretory Function of Microgel Coated $\beta$ -TC-6 Organoids

Insulin secretory responses of non-coated and coated  $\beta$ -TC-6 organoids were evaluated by static incubation of organoids in KRB with low and high glucose (LG and HG) concentration. LG and HG buffers were analyzed by insulin ELISA assay. Stimulation index (SI) was calculated for each group, by normalizing insulin amount in HG buffer to insulin amount in LG buffer. When SI value is higher than 1, insulin secretory response of islet to glucose is satisfactory and islets are considered functional.

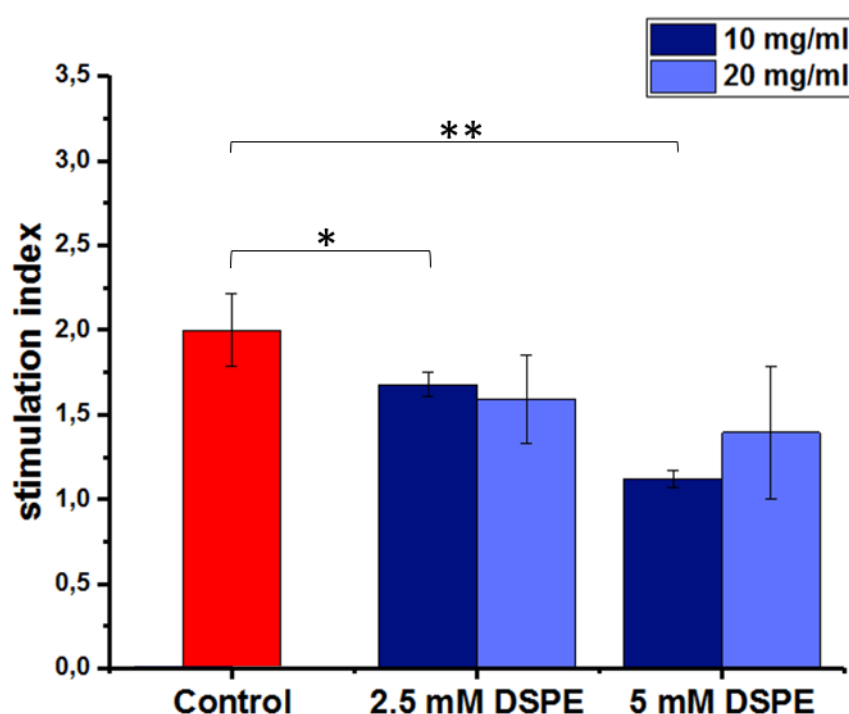


**Figure 4. 19.** Stimulation indices of  $\beta$ -TC-6 organoids after microgel treatment. SI values were calculated by dividing insulin level at high glucose to insulin level in low glucose buffer. Mean $\pm$ SD. \*\* $p$ <0.01. \* $p$ <0.05.

SI values were calculated as  $1,99\pm 0,21$ ,  $1,68\pm 0,07$ ,  $1,59\pm 0,26$ ,  $1,12\pm 0,05$  and  $1,39\pm 0,39$  for control, 2.5 mM DSPE/10mg/mL microgel, 2.5 mM DSPE/20 mg/ml microgel, 5 mM DSPE/10 mg/ml microgel and 5 mM DSPE/20 mg/ml microgel groups, respectively (**Figure 4.19**). All SI values were higher than 1, which indicates organoids were functional before and after microgel coating. Slight declines in SI when DSPE concentration in microgel is increased from 2.5 mM to 5 mM can be attributed to the fact that, when organoids are covered by more microgels in 5 mM

DSPE group, microgels might have interfered with insulin and glucose diffusion. All groups performed comparable after being challenged by different glucose levels and this indicates that microgel coating of organoids do not have adverse effect on islet function.



## Chapter 5

### **Conclusions and Future Work**

Islet transplantation for the treatment of T1D is a promising method, yet problems including immune responses, donor shortage and islet rejection/loss remains unsolved. In this thesis work, we have designed immunoisolation barriers for islets with two different concepts. Our biological concept utilized chemokines and immune cells to manipulate autoimmune reactions taking place in the body after islet transplantation. Specifically, we transfected HSCs with CCL22 chemokine, which is capable of recruiting suppressor Tregs. We prepared islet-mimicking structures, so called islet organoids, with insulin secreting  $\beta$ -TC-6 cells and CCL22 transfected-HSCs. After implantation of these multicellular organoids to diabetic mice, we observed high amount of Treg population around the implantation site. Recruitment of Tregs to implantation site provides an immune-privileged microenvironment for islets and may overcome islet rejection and loss of function. Our material-based concept consisted of synthesizing PEG-lipid microgels and coating of  $\beta$ -TC-6 organoids. Lipid-containing microgels were synthesized in mild conditions using W/W emulsion technique and visible light photopolymerization. Islet organoid coating was also achieved by a single step incubation of islet organoids in PEG-lipid microgel solution. Microgels of approximately 2-3  $\mu\text{m}$  diameter were anchored to islet surface via hydrophobic interactions, which is a harmless bonding method, compared to covalent interactions. For all conditions studied, we observed high viability and metabolic activities for coated islet organoids. Insulin secretory response to glucose was also similar to non-coated control organoids, which suggested that coating did not adversely affect islet function. To take this research one step forward, vascularization of implanted islets will be investigated. Additionally, for the reversal of diabetes, transplanted islets should be integrated to the implantation site and remain viable through blood supply from vasculature around them. For a prolonged islet survival in diabetic animal models, an improved engraftment of islets to the implantation site is essential. Therefore, different sites can be considered, such as kidney capsule which is

frequently used for islet transplantation studies with animal models. A hydrogel network composed of lipid groups for coating and proangiogenic factors such as VEGF can be utilized for an enhanced immunoisolation and survival of implanted islets, respectively. Also, combining biological and material-based strategies can be superior for islet transplantation technology. For example, coating multicellular islet organoids, composed of beta cells and HSCs, with PEG-lipid microgels can overcome islet rejection problems and contribute to islet survival, which can be considered as a future work in this study. In summary, to find an end-point solution to diabetes, the interactions between different cell types, functional biomaterials and islets should be thoroughly investigated through *in vitro* and *in vivo* experiments.



**BIBLIOGRAPHY**

1. Association, A.D., *Diagnosis and classification of diabetes mellitus*. Diabetes care, 2014. **37**(Supplement 1): p. S81-S90.
2. Samols, E., et al., *The order of islet microvascular cellular perfusion is B---A---D in the perfused rat pancreas*. The Journal of clinical investigation, 1988. **82**(1): p. 350-353.
3. Kepsutlu, B., et al., *Design of bioartificial pancreas with functional micro/nano-based encapsulation of islets*. Current pharmaceutical biotechnology, 2014. **15**(7): p. 590-608.
4. Robertson, R.P., *Islet transplantation as a treatment for diabetes—a work in progress*. New England Journal of Medicine, 2004. **350**(7): p. 694-705.
5. Matsumoto, S., *Islet cell transplantation for Type 1 diabetes*. Journal of diabetes, 2010. **2**(1): p. 16-22.
6. Berney, T. and A. Secchi, *Rapamycin in islet transplantation: friend or foe?* Transplant International, 2009. **22**(2): p. 153-161.
7. Scharp, D.W. and P. Marchetti, *Encapsulated islets for diabetes therapy: history, current progress, and critical issues requiring solution*. Advanced drug delivery reviews, 2014. **67**: p. 35-73.
8. Gołąb, K., et al. *Improved coating of pancreatic islets with regulatory T cells to create local immunosuppression by using the biotin-polyethylene glycol-succinimidyl valeric acid ester molecule*. in *Transplantation proceedings*. 2014. Elsevier.
9. Berman, D.M., et al., *Mesenchymal stem cells enhance allogeneic islet engraftment in nonhuman primates*. Diabetes, 2010.
10. Cameron, D.F., J.J. Hushen, and S.J. Nazian, *Formation of insulin-secreting, Sertoli-enriched tissue constructs by microgravity coculture of isolated pig islets and rat Sertoli cells*. In *Vitro Cellular & Developmental Biology-Animal*, 2001. **37**(8): p. 490-498.
11. Del Toro-Arreola, A., et al., *The role of endothelial cells on islet function and revascularization after islet transplantation*. Organogenesis, 2016. **12**(1): p. 28-32.
12. Efrat, S. and H.A. Russ, *Making  $\beta$  cells from adult tissues*. Trends in Endocrinology & Metabolism, 2012. **23**(6): p. 278-285.
13. Atkinson, M.A., G.S. Eisenbarth, and A.W. Michels, *Type 1 diabetes*. The Lancet, 2014. **383**(9911): p. 69-82.
14. Moltchanova, E., et al., *Seasonal variation of diagnosis of Type 1 diabetes mellitus in children worldwide*. Diabetic Medicine, 2009. **26**(7): p. 673-678.
15. Kahn, H.S., et al., *Association of type 1 diabetes with month of birth among US youth: The SEARCH for Diabetes in Youth Study*. Diabetes Care, 2009.
16. Noble, J.A., et al., *HLA class I and genetic susceptibility to type 1 diabetes: results from the Type 1 Diabetes Genetics Consortium*. Diabetes, 2010.
17. Patterson, C.C., et al., *Incidence trends for childhood type 1 diabetes in Europe during 1989–2003 and predicted new cases 2005–20: a multicentre prospective registration study*. The Lancet, 2009. **373**(9680): p. 2027-2033.

18. Thunander, M., et al., *Incidence of type 1 and type 2 diabetes in adults and children in Kronoberg, Sweden*. Diabetes research and clinical practice, 2008. **82**(2): p. 247-255.
19. Ehehalt, S., et al., *Prediction model for the incidence and prevalence of type 1 diabetes in childhood and adolescence: evidence for a cohort-dependent increase within the next two decades in Germany*. Pediatric diabetes, 2012. **13**(1): p. 15-20.
20. Polonsky, K.S., *The past 200 years in diabetes*. New England Journal of Medicine, 2012. **367**(14): p. 1332-1340.
21. Salsali, A. and M. Nathan, *A review of types 1 and 2 diabetes mellitus and their treatment with insulin*. American journal of therapeutics, 2006. **13**(4): p. 349-361.
22. Atkinson, M.A. and G.S. Eisenbarth, *Type 1 diabetes: new perspectives on disease pathogenesis and treatment*. The Lancet, 2001. **358**(9277): p. 221-229.
23. Im, G.-B. and S.H. Bhang, *Recent research trend in cell and drug delivery system for type 1 diabetes treatment*. Journal of Pharmaceutical Investigation, 2018: p. 1-11.
24. Kizilel, S., M. Garfinkel, and E. Opara, *The bioartificial pancreas: progress and challenges*. Diabetes technology & therapeutics, 2005. **7**(6): p. 968-985.
25. *United Network for Organ Sharing*. Retrieved from <https://www.unos.org/data>. 2016.
26. Morrison, H., *Contributions to the Microscopic Anatomy of the Pancreas, by PAUL LANGERHANS (Berlin 1869). With an English Translation and an Introductory Essay*. Bulletin of the History of Medicine, 1937. **5**: p. 259.
27. Ballinger, W.F. and P.E. Lacy, *Transplantation of intact pancreatic islets in rats*. Surgery, 1972. **72**(2): p. 175-186.
28. Scharp, D.W., et al., *Insulin independence after islet transplantation into type I diabetic patient*. Diabetes, 1990. **39**(4): p. 515-518.
29. Hering, B.J., et al., *Single-donor, marginal-dose islet transplantation in patients with type 1 diabetes*. Jama, 2005. **293**(7): p. 830-835.
30. Kojima, N., *In vitro reconstitution of pancreatic islets*. Organogenesis, 2014. **10**(2): p. 225-230.
31. Skelin, M., M. Rupnik, and A. Cencič, *Pancreatic beta cell lines and their applications in diabetes mellitus research*. ALTEX-Alternatives to animal experimentation, 2010. **27**(2): p. 105-113.
32. Bernard, A.B., C.-C. Lin, and K.S. Anseth, *A microwell cell culture platform for the aggregation of pancreatic  $\beta$ -cells*. Tissue Engineering Part C: Methods, 2012. **18**(8): p. 583-592.
33. Lin, R.Z. and H.Y. Chang, *Recent advances in three-dimensional multicellular spheroid culture for biomedical research*. Biotechnology Journal: Healthcare Nutrition Technology, 2008. **3**(9-10): p. 1172-1184.
34. Hwang, J.W., et al., *Functional clustering of pancreatic islet cells using concave microwell array*. Macromolecular research, 2011. **19**(12): p. 1320-1326.
35. Gao, B., et al., *Engineering of microscale three-dimensional pancreatic islet models in vitro and their biomedical applications*. Critical reviews in biotechnology, 2016. **36**(4): p. 619-629.

36. Lee, G.H., et al., *Bottom-Up Engineering of Well-Defined 3D Microtissues Using Microplatforms and Biomedical Applications*. *Advanced healthcare materials*, 2016. **5**(1): p. 56-74.
37. Ricordi, C., et al., *Human islet isolation and allotransplantation in 22 consecutive cases*. *Transplantation*, 1992. **53**(2): p. 407.
38. Hering, B., *Islet transplantation for patients with type 1 diabetes: results, research priorities, and reasons for optimism*. *Graft*, 1999. **2**: p. 12-27.
39. Ricordi, C., *Lilly Lecture 2002: Islet Transplantation: A Brave New World*. *Diabetes*, 2003. **52**(7): p. 1595-1603.
40. Fernandez, L.A., et al., *The Effects Of Maintenance Doses Of Fk506 Versus Cyclosporin A On Glucose And Lipid Metabolism After Orthotopic Liver Transplantation I*. *Transplantation*, 1999. **68**(10): p. 1532-1541.
41. Ryan, E.A., et al., *Successful islet transplantation: continued insulin reserve provides long-term glycemic control*. *Diabetes*, 2002. **51**(7): p. 2148-2157.
42. Narang, A.S. and R.I. Mahato, *Biological and biomaterial approaches for improved islet transplantation*. *Pharmacological reviews*, 2006. **58**(2): p. 194-243.
43. Solari, M.G., et al., *Marginal mass islet transplantation with autologous mesenchymal stem cells promotes long-term islet allograft survival and sustained normoglycemia*. *Journal of autoimmunity*, 2009. **32**(2): p. 116-124.
44. Chen, C.H., et al., *In vivo immune modulatory activity of hepatic stellate cells in mice*. *Hepatology*, 2006. **44**(5): p. 1171-1181.
45. Abdi, R., et al., *Immunomodulation by mesenchymal stem cells: a potential therapeutic strategy for type 1 diabetes*. *Diabetes*, 2008. **57**(7): p. 1759-1767.
46. Christiaens, V., et al., *Functional interactions between pancreatic beta cells and (pre) adipocytes*. *Endocrine*, 2010. **38**(1): p. 118-126.
47. Bloch, K., et al., *Immobilized microalgal cells as an oxygen supply system for encapsulated pancreatic islets: a feasibility study*. *Artificial organs*, 2006. **30**(9): p. 715-718.
48. Kojima, N., S. Takeuchi, and Y. Sakai. *Engineering of pseudoislets: effect on insulin secretion activity by cell number, cell population, and microchannel networks*. in *Transplantation proceedings*. 2014. Elsevier.
49. Lee, J.I., et al., *A newly developed immunoisolated bioartificial pancreas with cell sheet engineering*. *Cell transplantation*, 2008. **17**(1-2): p. 51-59.
50. Lee, J., et al. *Long-term viability of transplanted hybrid cellular spheroids within chondrocyte sheets*. in *Transplantation proceedings*. 2012. Elsevier.
51. Barba-Gutierrez, D.A., et al. *Facilitated Engraftment of Isolated Islets Coated With Expanded Vascular Endothelial Cells for Islet Transplantation*. in *Transplantation proceedings*. 2016. Elsevier.
52. Jaramillo, M. and I. Banerjee, *Endothelial cell co-culture mediates maturation of human embryonic stem cell to pancreatic insulin producing cells in a directed differentiation approach*. *Journal of visualized experiments: JoVE*, 2012(61).
53. Kang, S., et al., *Endothelial progenitor cell cotransplantation enhances islet engraftment by rapid revascularization*. *Diabetes*, 2012: p. DB\_101492.
54. Paget, M., et al., *Rotational co-culture of clonal  $\beta$ -cells with endothelial cells: effect of PPAR- $\gamma$  agonism in vitro on insulin and VEGF secretion*. *Diabetes, Obesity and Metabolism*, 2011. **13**(7): p. 662-668.

55. Sabra, G. and P. Vermette, *A 3D cell culture system: Separation distance between INS-1 cell and endothelial cell monolayers co-cultured in fibrin influences INS-1 cells insulin secretion*. *Biotechnology and bioengineering*, 2013. **110**(2): p. 619-627.
56. Spelios, M.G., et al., *In vitro formation of  $\beta$  cell pseudoislets using islet-derived endothelial cells*. *PloS one*, 2013. **8**(8): p. e72260.
57. Talavera-Adame, D., et al., *Effective endothelial cell and human pluripotent stem cell interactions generate functional insulin-producing beta cells*. *Diabetologia*, 2016. **59**(11): p. 2378-2386.
58. Takemoto, N., et al., *Transplantation of co-aggregates of Sertoli cells and islet cells into liver without immunosuppression*. *Transplantation*, 2014. **97**(3): p. 287-293.
59. Gressner, A. and R. Weiskirchen, *Modern pathogenetic concepts of liver fibrosis suggest stellate cells and TGF- $\beta$  as major players and therapeutic targets*. *Journal of cellular and molecular medicine*, 2006. **10**(1): p. 76-99.
60. Passino, M.A., et al., *Regulation of hepatic stellate cell differentiation by the neurotrophin receptor p75NTR*. *Science*, 2007. **315**(5820): p. 1853-1856.
61. Charles, R., et al., *Human Hepatic Stellate Cells Inhibit T cell Response through B7-H1 Pathway*. *Transplantation*, 2013. **96**(1): p. 17.
62. Jiang, G., et al., *Hepatic stellate cells preferentially expand allogeneic CD4+ CD25+ FoxP3+ regulatory T cells in an IL-2 dependent manner*. *Transplantation*, 2008. **86**(11): p. 1492.
63. Schildberg, F.A., et al., *Murine hepatic stellate cells veto CD8 T cell activation by a CD54-dependent mechanism*. *Hepatology*, 2011. **54**(1): p. 262-272.
64. Yang, H.R., et al., *Mechanistic insights into immunomodulation by hepatic stellate cells in mice: A critical role of interferon- $\gamma$  signaling*. *Hepatology*, 2009. **50**(6): p. 1981-1991.
65. Yang, H.R., et al., *A critical role of TRAIL expressed on cotransplanted hepatic stellate cells in prevention of islet allograft rejection*. *Microsurgery: Official Journal of the International Microsurgical Society and the European Federation of Societies for Microsurgery*, 2010. **30**(4): p. 332-337.
66. Masamune, A., et al., *Hypoxia stimulates pancreatic stellate cells to induce fibrosis and angiogenesis in pancreatic cancer*. *American Journal of Physiology-Gastrointestinal and Liver Physiology*, 2008. **295**(4): p. G709-G717.
67. Yin, Z., et al., *Cotransplanted hepatic stellate cells enhance vascularization of islet allografts*. *Microsurgery: Official Journal of the International Microsurgical Society and the European Federation of Societies for Microsurgery*, 2007. **27**(4): p. 324-327.
68. Ferretti, C. and A. La Cava, *Adaptive immune regulation in autoimmune diabetes*. *Autoimmunity reviews*, 2016. **15**(3): p. 236-241.
69. Barthlott, T., et al., *CD25+ CD4+ T cells compete with naive CD4+ T cells for IL-2 and exploit it for the induction of IL-10 production*. *International immunology*, 2005. **17**(3): p. 279-288.
70. Nishikawa, H. and S. Sakaguchi, *Regulatory T cells in cancer immunotherapy*. *Current opinion in immunology*, 2014. **27**: p. 1-7.
71. Miyara, M., Y. Ito, and S. Sakaguchi, *T REG-cell therapies for autoimmune rheumatic diseases*. *Nature Reviews Rheumatology*, 2014. **10**(9): p. 543.

72. Headen, D.M., et al., *Local immunomodulation with Fas ligand-engineered biomaterials achieves allogeneic islet graft acceptance*. Nature materials, 2018: p. 1.
73. Yoshie, O. and K. Matsushima, *CCR4 and its ligands: from bench to bedside*. International immunology, 2014. **27**(1): p. 11-20.
74. Montane, J., et al., *CCL22 prevents rejection of mouse islet allografts and induces donor-specific tolerance*. Cell transplantation, 2015. **24**(10): p. 2143-2154.
75. Montane, J., et al., *Prevention of murine autoimmune diabetes by CCL22-mediated Treg recruitment to the pancreatic islets*. The Journal of clinical investigation, 2011. **121**(8): p. 3024-3028.
76. Bal, T., et al., *Sequential Coating of Insulin Secreting Beta Cells within Multilayers of Polysaccharide Nanogels*. Macromolecular bioscience, 2018. **18**(5): p. 1800001.
77. Lim, F. and A.M. Sun, *Microencapsulated islets as bioartificial endocrine pancreas*. Science, 1980. **210**(4472): p. 908-910.
78. Iwata, H., et al., *Evaluation of microencapsulated islets in agarose gel as bioartificial pancreas by studies of hormone secretion in culture and by xenotransplantation*. Diabetes, 1989. **38**(Supplement 1): p. 224-225.
79. Zielinski, B.A. and P. Aebischer, *Chitosan as a matrix for mammalian cell encapsulation*. Biomaterials, 1994. **15**(13): p. 1049-1056.
80. Riopel, M. and R. Wang, *Collagen matrix support of pancreatic islet survival and function*. Front Biosci, 2014. **19**(1): p. 77-90.
81. Cruise, G.M., et al., *In Vitro and In Vivo Performance of Porcine Islets Encapsulated in Interfacially Photopolymerized Poly (Ethylene Glycol) Diacrylate Membranes*. Cell transplantation, 1999. **8**(3): p. 293-306.
82. Govan, J., J. Fyfe, and T. Jarman, *Isolation of alginate-producing mutants of Pseudomonas fluorescens, Pseudomonas putida and Pseudomonas mendocina*. Microbiology, 1981. **125**(1): p. 217-220.
83. Van Schilfgaarde, R. and P. De Vos, *Factors influencing the properties and performance of microcapsules for immunoprotection of pancreatic islets*. Journal of molecular medicine, 1999. **77**(1): p. 199-205.
84. Skjåk-Bræk, G., E. Murano, and S. Paoletti, *Alginate as immobilization material. II: Determination of polyphenol contaminants by fluorescence spectroscopy, and evaluation of methods for their removal*. Biotechnology and bioengineering, 1989. **33**(1): p. 90-94.
85. Soon-Shiong, P., et al., *Insulin independence in a type 1 diabetic patient after encapsulated islet transplantation*. The Lancet, 1994. **343**(8903): p. 950-951.
86. Calafiore, R., et al., *Microencapsulated pancreatic islet allografts into nonimmunosuppressed patients with type 1 diabetes: first two cases*. Diabetes care, 2006. **29**(1): p. 137-138.
87. Elliott, R., et al. *Intraperitoneal alginate-encapsulated neonatal porcine islets in a placebo-controlled study with 16 diabetic cynomolgus primates*. in *Transplantation proceedings*. 2005. Elsevier.
88. Elliott, R.B., et al. *Transplantation of Microencapsulated Neonatal Porcine Islets in Patients with Type 1 Diabetes: Safety and Efficacy*. in *Diabetes*. 2010. AMER DIABETES ASSOC 1701 N BEAUREGARD ST, ALEXANDRIA, VA 22311-1717 USA.

89. Elliott, R.B., et al., *Live encapsulated porcine islets from a type 1 diabetic patient 9.5 yr after xenotransplantation*. *Xenotransplantation*, 2007. **14**(2): p. 157-161.
90. Hernández, R.M., et al., *Microcapsules and microcarriers for in situ cell delivery*. *Advanced drug delivery reviews*, 2010. **62**(7-8): p. 711-730.
91. Tashiro, H., et al. *Application of agarose microcapsules to allo-islet transplantation in a canine model*. in *Transplantation proceedings*. 1998. Elsevier Science Publishing Company, Inc.
92. Kim, I.-Y., et al., *Chitosan and its derivatives for tissue engineering applications*. *Biotechnology advances*, 2008. **26**(1): p. 1-21.
93. Yang, K.-C., et al., *The cytoprotection of chitosan based hydrogels in xenogeneic islet transplantation: An in vivo study in streptozotocin-induced diabetic mouse*. *Biochemical and biophysical research communications*, 2010. **393**(4): p. 818-823.
94. Erkoc, P., et al., *Quinacrine Mediated Sensitization of Glioblastoma (GBM) Cells to TRAIL through MMP-Sensitive PEG Hydrogel Carriers*. *Macromolecular bioscience*, 2017. **17**(2): p. 1600267.
95. Bal, T., et al., *Mesenchymal stem cells and ligand incorporation in biomimetic poly (ethylene glycol) hydrogels significantly improve insulin secretion from pancreatic islets*. *Journal of tissue engineering and regenerative medicine*, 2017. **11**(3): p. 694-703.
96. Cinay, G.E., et al., *Nanogel-integrated pH-responsive composite hydrogels for controlled drug delivery*. *ACS Biomaterials Science & Engineering*, 2017. **3**(3): p. 370-380.
97. Aydin, D. and S. Kizilel, *P2X7 receptor antagonist delivery vehicle based on photocrosslinked amphiphilic hybrid gels*. *RSC Advances*, 2018. **8**(33): p. 18216-18226.
98. Okur, A.C., P. Erkoc, and S. Kizilel, *Targeting cancer cells via tumor-homing peptide CREKA functional PEG nanoparticles*. *Colloids and Surfaces B: Biointerfaces*, 2016. **147**: p. 191-200.
99. Aydin, D. and S. Kizilel, *Water-in-Water Emulsion Based Synthesis of Hydrogel Nanospheres with Tunable Release Kinetics*. *JOM*, 2017. **69**(7): p. 1185-1194.
100. Kizilel, S., V.H. Pérez-Luna, and F. Teymour, *Photopolymerization of poly (ethylene glycol) diacrylate on eosin-functionalized surfaces*. *Langmuir*, 2004. **20**(20): p. 8652-8658.
101. Ifkovits, J.L. and J.A. Burdick, *Photopolymerizable and degradable biomaterials for tissue engineering applications*. *Tissue engineering*, 2007. **13**(10): p. 2369-2385.
102. Teramura, Y. and H. Iwata, *Islets surface modification prevents blood-mediated inflammatory responses*. *Bioconjugate chemistry*, 2008. **19**(7): p. 1389-1395.
103. Lanza, R.P., J.L. Hayes, and W.L. Chick, *Encapsulated cell technology*. *Nature biotechnology*, 1996. **14**(9): p. 1107.
104. Vaithilingam, V., S. Bal, and B. Tuch, *Encapsulated Islet Transplantation: Where Do We Stand? The review of diabetic studies: RDS*, 2017. **14**(1): p. 51-78.

105. Safley, S.A., et al., *Biocompatibility and immune acceptance of adult porcine islets transplanted intraperitoneally in diabetic NOD mice in calcium alginate poly-L-lysine microcapsules versus barium alginate microcapsules without poly-L-lysine*. 2008, SAGE Publications.
106. Sun, Y., et al., *Normalization of diabetes in spontaneously diabetic cynomolgus monkeys by xenografts of microencapsulated porcine islets without immunosuppression*. The Journal of clinical investigation, 1996. **98**(6): p. 1417-1422.
107. Wang, T., et al., *Successful allotransplantation of encapsulated islets in pancreatectomized canines for diabetic management without the use of immunosuppression*. Transplantation, 2008. **85**(3): p. 331-337.
108. Basta, G., et al., *Long-term metabolic and immunological follow-up of nonimmunosuppressed patients with type 1 diabetes treated with microencapsulated islet allografts: four cases*. Diabetes care, 2011: p. DC\_110731.
109. Teramura, Y., et al., *Microencapsulation of cells, including islets, within stable ultra-thin membranes of maleimide-conjugated PEG-lipid with multifunctional crosslinkers*. Biomaterials, 2013. **34**(11): p. 2683-2693.
110. Kizilel, S., et al., *Encapsulation of pancreatic islets within nano-thin functional polyethylene glycol coatings for enhanced insulin secretion*. Tissue Engineering Part A, 2010. **16**(7): p. 2217-2228.
111. Teramura, Y. and H. Iwata, *Islet encapsulation with living cells for improvement of biocompatibility*. Biomaterials, 2009. **30**(12): p. 2270-2275.
112. Esquena, J., *Water-in-water (W/W) emulsions*. Current Opinion in Colloid & Interface Science, 2016. **25**: p. 109-119.
113. Poortinga, A.T., *Microcapsules from self-assembled colloidal particles using aqueous phase-separated polymer solutions*. Langmuir, 2008. **24**(5): p. 1644-1647.
114. Gonzalez-Jordan, A., T. Nicolai, and L. Benyahia, *Influence of the protein particle morphology and partitioning on the behavior of particle-stabilized water-in-water emulsions*. Langmuir, 2016. **32**(28): p. 7189-7197.
115. Nguyen, B.T., et al., *pH-responsive water-in-water Pickering emulsions*. Langmuir, 2015. **31**(12): p. 3605-3611.
116. Stokes, J., B. Wolf, and W. Frith, *Phase-separated biopolymer mixture rheology: Prediction using a viscoelastic emulsion model*. Journal of Rheology, 2001. **45**(5): p. 1173-1191.
117. Padilha, G.d.S., et al., *Extraction of lipase from Burkholderia cepacia by PEG/Phosphate ATPS and its biochemical characterization*. Brazilian Archives of biology and Technology, 2012. **55**(1): p. 7-19.
118. Norton, J., et al., *Functional food microstructures for macronutrient release and delivery*. Food & function, 2015. **6**(3): p. 663-678.
119. Dickinson, E., *Exploring the frontiers of colloidal behaviour where polymers and particles meet*. Food Hydrocolloids, 2016. **52**: p. 497-509.
120. Fernández-Barbero, A., et al., *Gels and microgels for nanotechnological applications*. Advances in colloid and interface science, 2009. **147**: p. 88-108.
121. Franssen, O. and W.E. Hennink, *A novel preparation method for polymeric microparticles without the use of organic solvents*. International Journal of Pharmaceutics, 1998. **168**(1): p. 1-7.

122. Buzza, D.M.A., et al., *Water-in-Water Emulsions Based on Incompatible Polymers and Stabilized by Triblock Copolymers–Templated Polymersomes*. Langmuir, 2013. **29**(48): p. 14804-14814.
123. Belair, D.G., et al., *Serum-dependence of affinity-mediated VEGF release from biomimetic microspheres*. Biomacromolecules, 2014. **15**(6): p. 2038-2048.
124. Belair, D.G., N.N. Le, and W.L. Murphy, *Regulating VEGF signaling in platelet concentrates via specific VEGF sequestering*. Biomaterials science, 2016. **4**(5): p. 819-825.
125. Belair, D.G., et al., *Differential regulation of angiogenesis using degradable VEGF-binding microspheres*. Biomaterials, 2016. **93**: p. 27-37.
126. Impellitteri, N.A., et al., *Specific VEGF sequestering and release using peptide-functionalized hydrogel microspheres*. Biomaterials, 2012. **33**(12): p. 3475-3484.
127. Parlato, M., et al., *Adaptable poly (ethylene glycol) microspheres capable of mixed-mode degradation*. Acta biomaterialia, 2013. **9**(12): p. 9270-9280.
128. Sutherland, D., R. Stratta, and A. Gruessner, *Pancreas transplant outcome by recipient category: single pancreas versus combined kidney-pancreas*. Curr Opin Organ Transplant, 1998. **3**: p. 231-241.
129. London, N., *Clinical studies of human islet transplantation*. Annals of the Royal College of Surgeons of England, 1995. **77**(4): p. 263.
130. Bynigeri, R.R., et al., *Pancreatic stellate cell: Pandora's box for pancreatic disease biology*. World journal of gastroenterology, 2017. **23**(3): p. 382.
131. MacDonald, K.G., P.C. Orban, and M.K. Levings, *T regulatory cell therapy in transplantation: stability, localization and functional specialization*. Current opinion in organ transplantation, 2012. **17**(4): p. 343-348.
132. Shapiro, A.J., et al., *International trial of the Edmonton protocol for islet transplantation*. New England Journal of Medicine, 2006. **355**(13): p. 1318-1330.
133. Shapiro, A.J., M. Pokrywczynska, and C. Ricordi, *Clinical pancreatic islet transplantation*. Nature Reviews Endocrinology, 2017. **13**(5): p. 268.
134. Van Der Windt, D.J., et al., *Rapid loss of intraportally transplanted islets: an overview of pathophysiology and preventive strategies*. Xenotransplantation, 2007. **14**(4): p. 288-297.
135. Bechstein, W.O., *Neurotoxicity of calcineurin inhibitors: impact and clinical management*. Transplant International, 2000. **13**(5): p. 313-326.
136. Randhawa, P.S., T.E. Starzl, and A.J. Demetris, *Tacrolimus (FK506)-associated renal pathology*. Advances in anatomic pathology, 1997. **4**(4): p. 265.
137. Persaud, S.J., et al., *Pseudoislets as primary islet replacements for research: report on a symposium at King's College London, London UK*. Islets, 2010. **2**(4): p. 236-239.
138. Persaud, S.J., *PANCREATIC B-CELL LINES*. The Biology of the Pancreatic Cell, 1999. **29**: p. 21.
139. Vermonden, T., et al., *Photopolymerized thermosensitive hydrogels: synthesis, degradation, and cytocompatibility*. Biomacromolecules, 2008. **9**(3): p. 919-926.
140. Rabanel, J.M., et al., *Progress technology in microencapsulation methods for cell therapy*. Biotechnology progress, 2009. **25**(4): p. 946-963.

141. Miura, S., Y. Teramura, and H. Iwata, *Encapsulation of islets with ultra-thin polyion complex membrane through poly (ethylene glycol)-phospholipids anchored to cell membrane*. *Biomaterials*, 2006. **27**(34): p. 5828-5835.
142. Inui, O., Y. Teramura, and H. Iwata, *Retention dynamics of amphiphilic polymers PEG-lipids and PVA-alkyl on the cell surface*. *ACS applied materials & interfaces*, 2010. **2**(5): p. 1514-1520.
143. Teramura, Y. and H. Iwata, *Surface modification of islets with PEG-lipid for improvement of graft survival in intraportal transplantation*. *Transplantation*, 2009. **88**(5): p. 624-630.
144. Teramura, Y. and H. Iwata, *Improvement of graft survival by surface modification with poly (ethylene glycol)-lipid and urokinase in intraportal islet transplantation*. *Transplantation*, 2011. **91**(3): p. 271-278.
145. Teramura, Y., et al., *Behavior of synthetic polymers immobilized on a cell membrane*. *Biomaterials*, 2008. **29**(10): p. 1345-1355.
146. Vabbilisetty, P., et al., *Chemical Reactive Anchoring Lipids with Different Performance for Cell Surface Re-engineering Application*. *ACS omega*, 2018. **3**(2): p. 1589-1599.
147. Dong, H., et al., *Immuno-isolation of pancreatic islet allografts using pegylated nanotherapy leads to long-term normoglycemia in full MHC mismatch recipient mice*. *PloS one*, 2012. **7**(12): p. e50265.
148. Forciniti, D., C. Hall, and M. Kula, *Interfacial tension of polyethyleneglycol-dextran-water systems: influence of temperature and polymer molecular weight*. *Journal of Biotechnology*, 1990. **16**(3-4): p. 279-296.
149. Maggioris, D., et al., *Prediction of particle size distribution in suspension polymerization reactors: effect of turbulence nonhomogeneity*. *Chemical Engineering Science*, 2000. **55**(20): p. 4611-4627.
150. Bastiancich, C., et al., *Anticancer drug-loaded hydrogels as drug delivery systems for the local treatment of glioblastoma*. *Journal of Controlled Release*, 2016. **243**: p. 29-42.
151. Zhou, D., et al., *In vitro and in vivo evaluation of insulin-producing  $\beta$ TC6-F7 cells in microcapsules*. *American Journal of Physiology-Cell Physiology*, 1998. **274**(5): p. C1356-C1362.
152. Pethig, R., et al., *Dielectrophoretic assembly of insulinoma cells and fluorescent nanosensors into three-dimensional pseudo-islet constructs*. *IET nanobiotechnology*, 2008. **2**(2): p. 31-38.
153. Petry, F., et al., *Three-Dimensional Bioreactor Technologies for the Cocultivation of Human Mesenchymal Stem/Stromal Cells and Beta Cells*. *Stem cells international*, 2018. **2018**.
154. Samuelson, L. and D.A. Gerber, *Improved function and growth of pancreatic cells in a three-dimensional bioreactor environment*. *Tissue Engineering Part C: Methods*, 2012. **19**(1): p. 39-47.
155. Atchison, N., et al., *Maintenance of ischemic  $\beta$  cell viability through delivery of lipids and ATP by targeted liposomes*. *Biomaterials science*, 2014. **2**(4): p. 548-559.